Journal of Comparative Neurology

WILEY

JCN RESEARCH IN SYSTEMS NEUROSCIENCE THE JOURNAL OF COMPARATIVE NEUROLOGY

RESEARCH ARTICLE OPEN ACCESS

Atypical Course of the Habenulo-Interpeduncular Tract in Chick Embryos

José Luis Ferran[1,2] | Luis Puelles[1,2]

[1]Department of Human Anatomy and Psychobiology, Faculty of Medicine, University of Murcia, Murcia, Spain | [2]Pascual Parrilla Institute of Biomedical Research of Murcia, Virgen de la Arrixaca University Hospital, Murcia, Spain

Correspondence: José Luis Ferran (jlferran@um.es)

Received: 28 January 2024 | **Revised:** 15 April 2024 | **Accepted:** 30 May 2024

Funding: This study was funded by the Spanish Ministry of Science, Innovation and Universities (MCIU), State Research Agency (AEI) and European Regional Development Fund (FEDER) (Grant PGC2018-098229-B-100 to JLF) and by Séneca Foundation (Grants 19904/GERM/15 and 21903/PI/22).

Keywords: interpeduncular nucleus | lateral habenula | medial habenula | prosomere 2 | retroflex tract

ABSTRACT

Classical studies of the avian diencephalon hardly mention the habenulo-interpeduncular tract (a.k.a. retroflex tract), although both the habenula (HB) (its origin) and the interpeduncular nuclear complex (its target) are present. Retroflex tract fibers were described at early embryonic stages but seem absent in the adult in routine stains. However, this tract is a salient diencephalic landmark in all other vertebrate lineages. It typically emerges out of the caudal HB, courses dorsoventrally across thalamic alar and basal plates just in front of the thalamo-pretectal boundary, and then sharply bends 90° caudalwards at paramedian basal plate levels (this is the "retroflexion"), to approach longitudinally via paramedian pretectum and midbrain the rostralmost hindbrain, specifically the prepontine median interpeduncular complex across isthmus and rhombomere 1. We systematize this habenulo-interpeduncular course into four parts named subhabenular, retrothalamic, tegmental, and interpeduncular. We reexamined the chicken habenulo-interpeduncular fibers at stages HH30 and HH35 (6.5- and 9-day incubation) by mapping them specifically with immunoreaction for BEN protein, a well-known marker. We found that only a small fraction of the stained retroflex tract fibers approaches the basal plate by coursing along the standard dorsoventral pathway in front of the thalamo-pretectal boundary. Many other habenular fibers instead diverge into atypical dispersed courses across the thalamic cell mass (implying alteration of the first subhabenular part of the standard course) before reaching the basal plate; this dispersion explains their invisibility. A significant number of such transthalamic habenular fibers cross orthogonally the zona limitans (ZLI) (the rostral thalamic boundary) and invade the caudal alar prethalamus. Here, they immediately descend dorsoventrally, just rostrally to the ZLI, until reaching the prethalamic basal plate, where they bend (retroflex) caudalwards, entering the thalamic basal paramedian area. These atypical fibers gradually fasciculate with the other groups of habenular efferent fibers in their final longitudinal approach to the hindbrain interpeduncular complex. We conclude that the poor visibility of this tract in birds is due to its dispersion into a diversity of atypical

Abbreviations: III, oculomotor nucleus and nerve; IV, trochlear nucleus and nerve; IVv, four ventricle; Cer, cerebellum; cf, cephalic flexure; ch, optic chiasma; Dien, diencephalon; dt, dorsal tier; DCa, dorsocaudal nucleus; DF, Dorsofrontal nucleus; DF/DCa, Dorsofrontal/Dorsocaudal nuclei; dtgd, Dorsal tegmental decussation of the midbrain; DTh, Dorsal thalamus (columnar); ep, epiphysis; ETh, epithalamus (columnar); flm, fasciculus longitudinalis medialis; FP, floor plate; HB, habenula; Ist, isthmic region; Isth. Nn, isthmic nuclei; hp1, hypothalamo-telencephalic prosomere 1; hp2, hypothalamo-telencephalic prosomere 2; HTh, hypothalamus; IC, inferior colliculus; IP, interpeduncular nucleus complex; it, intermediate tier; ma, mamillary body; m1, mesomere 1; m2, mesomere 2; Med, medulla Oblongata; Mes, mesencephalon; MT, medial terminal nucleus; p1, diencephalic prosomere 1; p2, diencephalic prosomere 2; p3, diencephalic prosomere 3; PHTh, posterior Hypothalamus (columnar); PHy, peduncular Hypothalamus (prosomeric); Poa, preoptic area; PT, pretectum; PTh, prethalamus; r0-r11, rhombomeres r0 to r11; rf, retroflex tract; rff, retroflex tract field; Romb, rombencephalon; SC, superior colliculus; SCo, spinal cord; Sec. Pros., secondary prosencephalon; SL, semilunaris nucleus; SPT, subpretectal nucleus; STh, subthalamic nucleus; Tel, Telencephalon; TG, midbrain tectal gray; Th, thalamus (prosomeric); tth, tecto-thalamic tract; THy, terminal Hypothalamus (prosomeric); VTh, ventral thalamus (columnar); vt, ventral tier; ZLI, zona limitans intrathalamica.

alternative routes, though all components eventually reach the interpeduncular complex. This case merits further analysis of the diverse permissive versus nonpermissive guidance mechanisms called into action, which partially correlate distinctly with successive diencephalic, mesencephalic, and hindbrain neuromeric fields and their boundaries.

1 | Introduction

The retroflex or habenulo-interpeduncular tract is a classically well-known anatomic landmark in the diencephalon (Dien) of vertebrates (Beccari 1923, 1943; Edinger 1908; Kappers, Huber, and Crosby 1936; Kuhlenbeck 1973, 1977; Nieuwenhuys, ten Donkelaar, and Nicholson 1998). It is formed essentially by efferent fibers of the medial and lateral habenular nuclei (found dorsal to the thalamic complex), which target, after a characteristic course, the hindbrain interpeduncular complex (and also other neighboring cell populations, including dopaminergic and serotonergic centers; Herkenham and Nauta 1979). The tract also contains minor ascending or descending contributions from opportunistic brainstem pathways, such as dopaminergic fibers from the interfascicular nucleus or histaminergic, serotonergic, and noradrenergic fibers (Loonen and Ivanova 2016; Schmidt et al. 2014). Normally, the habenular efferent fibers originated most rostrally gradually collect caudalwards under the habenula (HB) (a longitudinal trajectory), where they are joined by the more caudal counterparts. The increasing packet of subhabenular fibers proceeds caudalwards until its progress under the HB, and the thalamic retrohabenular area is apparently blocked by the habenulo-pretectal boundary (dorsal part of the interneuromeric thalamo-pretectal limit; Funato, Saito-Nakazato, and Takahashi 2000). At this point, the tract turns ventralwards and becomes a compact descending fiber packet that courses dorsoventrally through the caudalmost part of the thalamic alar plate, invading the hiatus existing between the caudal pole of the thalamus and the precommissural pretectum (i.e., passing just in front of the diencephalic prosomere 2 (p2)/p1 interprosomeric boundary). The position of the tract in the thalamic mantle zone is periventricular, not far from the ventricular lining. Once the dorsoventral course reaches the underlying thalamic basal plate (caudal part of p2 tegmentum), the tract continues its straight dorsoventral trajectory and approaches the local p2 floor plate (FP). Within this basal sector, the tract is crossed medially by the longitudinal mamillotegmental tract and limits rostrally the parvocellular red nucleus of the pretectal tegmentum (a characteristic property first described classically in the human brain). Having reached the paramedian part of the thalamic basal plate, the tract bends in a right angle near the basal-floor limit, continuing thereafter caudalwards. It courses longitudinally through the paramedian pretectal and mesencephalic tegmentum, parallel to the FP (see Moreno-Bravo et al. 2016). Finally, the tract crosses the isthmo-mesencephalic border in the same paramedian basal position and enters, ipsilaterally, the rostral pole of the interpeduncular complex. The latter develops across the floorplate of the isthmus (rhombomere 0) and rostral and caudal parts of rhombomere 1 (Lorente-Cánovas et al. 2012; Moreno-Bravo et al. 2014, 2016; Puelles 2016, 2019; Puelles, Watson et al. 2012; Puelles, Martinez-de-la-Torre et al. 2012). Note the classic literature sometimes wrongly ascribes other more rostral positions—such as a midbrain or even a diencephalic locus—to this nuclear complex due to erroneous delimitation of the midbrain. The terminal branches of the retroflex tract associated with the median and paramedian interpeduncular terminal field typically zigzag several times from left to right across the interpeduncular complex (and vice versa) as they gradually extend caudalwards through its median and paramedian parts (see his Fig.507; Iwahori, Nakamura, and Kameda 1993; Ramón y Cajal 1911); however, some collateral branches apparently follow simpler ipsilateral longitudinal trajectories to particular subnuclei or other targets (Contestabile et al. 1987; Groenewegen et al. 1986).

It is remarkable that the retroflex tract, though very distinct in all vertebrates (except possibly in frogs; Freudenmacher, von Twickel, and Walkowiak 2020), is normally not identified along a typical course in young postnatal or adult avian brains (e.g., den Boer-Visser, Brittijn, and Dubbeldam 2004; Karten and Hodos 1967; Kuenzel and Masson 1988; Medina and Reiner 1994; Puelles et al. 2007, 2019; Zweers 1971). However, both the habenular and interpeduncular complexes are well developed, and both are structurally similar to the counterparts in other vertebrates (Lorente-Cánovas et al. 2012; Puelles et al. 2007, 2019). Huber and Crosby (1929) identified in their Figs.40 and 41 the initial subhabenular course of the avian retroflex tract after staining it with reduced pyridine-silver in the dove brain (data later reproduced by Kappers, Huber, and Crosby 1936 in their Fig.494). These authors described the tract as divided into a lateral part, which occupies largely a standard retrothalamic position, behind the rotundus and triangularis thalamic nuclei, and a medial part, which seems to "cut straight through the dorsal thalamus." Though initially dispersed in this fashion, both moieties of the dove retroflex tract finally seem to reach the interpeduncular nucleus (Huber and Crosby 1929). Medina and Reiner (1994) reported expression of ChAT in the adult pigeon medial habenular nucleus and corresponding fibers in the retroflex tract (first three schemata of their Fig. 6); they did not comment about any abnormal course (see Section 4). Redies, Arndt, and Ast (1997), using selective anti-axonin-1 immunocytochemistry, reported massive staining of the chicken retroflex tract at stage HH34 (8 days in ovo; their Fig. 13C). These authors interpreted their data as indicating a standard retrothalamic course of the tract parallel to the thalamo-pretectal boundary, though their published images likewise suggest, in our opinion, some fibers penetrating the thalamus, as pointed out by Huber and Crosby (1929). The initial part of the chicken retroflex tract was also observed more recently in a coronal anti-calbindin immunoreacted section through a postnatal chick brain, as the tract just emerges out of the HB, but the subsequent course was not followed (Ferran et al. 2009; their Fig. 2B; see also the chick atlas of Puelles et al. 2007, 2019; e.g., their plates 76, 77). Guillén-Pérez (1991) apparently first noticed calbindin immunoreaction in this tract in her doctoral thesis, but she did not follow its complete course either.

In contrast, several studies centered on early chick embryos succeeded in identifying the retroflex tract. A handful of neurofibrillary studies reported the embryonic retroflex tract but unfortunately did not document these observations other than schematically (e.g., Beccari 1923; Bösel 1974; Lyser 1966; Tello 1924; Windle and Austin 1936). More recently, Chédotal, Pourquié, and Sotelo (1995) selectively stained pioneering retroflex tract fibers in chick embryos at stages HH20–HH22, using anti-BEN immunocytochemistry as a selective marker (Figures 5a, 6a, and 7c,d). These results also, show in retrospect, some indications of a defasciculated transthalamic course.

This analysis of the limited relevant literature suggests that there clearly exists a recognizable avian retroflex or habenulo-interpeduncular tract at early and middle embryonic stages, as well as at early postnatal stages. However, the obvious difficulties in identifying this tract in adult avian brains with standard histologic techniques (e.g., its being completely inconspicuous in Nissl material, in contrast to the case of most other vertebrates), taken together with the medial and lateral tract components described by Huber and Crosby (1929) with pyridine-silver, suggest partial defasciculation of its fibers into transthalamic courses. We report here results from a study examining the chicken retroflex tract at intermediate embryonic stages (HH30 and HH35; i.e., 6.5 and 9 days of incubation, respectively), using anti-BEN immunoreaction as a selective marker (Chédotal, Pourquié, and Sotelo 1995; Pourquié et al. 1990) and various counterstains. These data throw light about the atypical characteristics of the retroflex tract course in the chicken. A preliminary pair of images of the present study appeared in the second edition of the chick brain stereotaxic atlas (Puelles et al. 2019; their text Figure 19).

We found that only a fraction of the fibers of this tract follow a standard dorsoventral pathway into the p2 tegmentum coursing in front of the thalamo-pretectal boundary before bending caudalwards to reach longitudinally the hindbrain interpeduncular complex. Most habenular efferent fibers are diverted instead into dispersed atypical courses that traverse the thalamic cell mass in an *oblique* or even *rostrad* direction. Indeed, some of these trans-thalamic elements exit the thalamus rostralward and penetrate the alar prethalamus, thereafter bending ventralwards into the underlying p3 tegmentum. Here, they turn (retroflex) caudalwards and finally fasciculate with the other retroflex tract components coursing longitudinally through the diencephalic and midbrain paramedian tegmentum. The reunited retroflex tract finally enters, in a standard fashion, the interpeduncular complex located in the rostral hindbrain (isthmus and rhombomere 1).

2 | Materials and Methods

All experimental protocols and our use and care of laboratory animals were conducted in accordance with the current normative standards of the European Community (86/609/EEC) and the Spanish government (Royal Decree, 1201/2005; Law 32/2007). Our procedures were approved by the University of Murcia committee for ethical use of experimental animals.

2.1 | Animals and Tissue Preparation

All brain processing procedures were performed according to Ferran et al. (2015a, 2015b). Commercial fertilized chicken eggs (*Gallus gallus domesticus*, RRID:NCBITaxon_9031) were obtained from a national farm (Granja Santa Isabel; Córdoba, Spain). They were incubated in a forced draft incubator with slow basculation movements at 38°C, with 65% controlled humidity until they reached the desired stages (HH30, HH35, and HH36—staging proceeded according to Hamburger and Hamilton 1951). For comparison, several Swiss albino mouse embryos were collected at embryonic day (E) 16.5 after fertilization (vaginal plug taken as E0.5). Mice embryos (RRID:MGI_5652853) and the smaller chicken embryos were fixed by immersion during 16 h at 4°C in freshly prepared 4% paraformaldehyde in 0.1 M phosphate-buffered saline (PBS, pH 7.4); stage HH36 chicken embryos were perfused transcardially with the same solution under anesthesia. The brains were extracted shortly afterward and were postfixed with gentle agitation in the same cold fixative overnight. On the following day, the brains were washed three times (30 min each in pH 7.4 PBS at room temperature). The brains were next embedded in 4% low-melting point agarose in PBS (Pronadisa, Torrejón de Ardoz, Madrid, Spain, Cat. 8008) and cut on a Leica VT1000S vibratome (RRID:SCR_016495) 100–120 μm-thick in sagittal and transverse section planes relative to the thalamo-pretectal boundary region. The sections were subsequently processed as floating sections for in situ hybridization and/or immunohistochemistry, as described Ferran et al. (2015b).

2.2 | Reverse Transcription-Polymerase Chain Reaction (PCR)

In order to aid the search of the retroflex tract in its thalamic course, we mapped the thalamic marker gene *Tcf7l2* in both mouse and chicken material. The chicken probe plasmid was kindly given to us by H. Nakamura (see below), and we cloned the corresponding mouse probe. cDNA fragments from the mouse *Tcf7l2* gene were obtained by reverse transcription (RT). RNA was extracted from freshly dissected E16.5 mouse brains with Trizol reagent (Invitrogen, Carlsbad, CA, Cat. 10296-028) and was quickly frozen over dry ice. RNA was next treated with DNase I (Invitrogen, Cat. 18068-015) at room temperature to eliminate DNA, and the enzyme was next inactivated at 65°C during 5 min. The clean RNA was reverse-transcribed into single-stranded cDNA with superscript oculomotor nucleus and nerve (III) reverse transcriptase (Invitrogen, Cat. 18080-044) and oligo-dorsal tier (dt)-anchored primers. The resulting first-strand cDNA (0.5 μL of the RT reaction) was used as a template for the PCR reaction, performed with Taq polymerase (Promega, Cat.M8305), using the following specific primers:

mTcf7l2F: 5′-AAAATGCCGCAGCTGAACGG-3′

mTcf7l2R: 5′-GTCAGCGCTGTGGGGTAGGG-3′

The PCR reaction comprised denaturalization for 5 min at 94°C, followed by 35 cycles [30 s at 94°C, plus 1 min at Tm temperature (58°C), and 1 min at 72°C] and a final extension step at 72°C

for 20 min. The PCR products were cloned into pGEM-T Easy Vector (Promega, Cat. A1360) and sequenced (SAI, University of Murcia); we obtained a mTcf7l2 fragment of 788 bp (528-1316; with a NCBI accession number: NM_001142923.2).

2.3 | In Situ Hybridization

We used for in situ hybridization our own mouse *Tcf7l2* cDNA fragment as well as a chicken *Tcf7l2* cDNA provided by Dr. Nakamura (reference in Merchán et al. 2011), *FoxP2* (reference in Ferran et al. 2009), *Mes1* (reference in Sánchez-Guardado et al. 2011), and *Pax6* (reference in Merchán et al. 2011). All cDNAs used in this work were sequenced (SAI, University of Murcia), and their specificity was checked using the BLAST tool (NCBI). The antisense digoxigenin-labeled riboprobes for chicken (*Tcf7l2*, *FoxP2, Meis1, and Pax6*) and mouse *Tcf7l2* were synthesized with a Roche kit, following the manufacturer's recommendations (Roche Diagnostics S.L., Applied Science, Barcelona, Spain), and specific polymerases were applied (Fermentas, Madrid, Spain). The chicken and mouse brain vibratome sections were hybridized with digoxigenin-UTP-labeled antisense riboprobes according to the floating-section protocol of Ferran et al. (2015b). To detect the hybridized product, the sections were incubated overnight at 4°C with alkaline phosphatase-conjugated anti-digoxigenin Fab fragments (1:3500, Roche Cat# 11093274910, RRID:AB_51449), and nitroblue tetrazolium/bromochloroindolyl phosphate was used as chromogenic substrate for the final alkaline phosphatase reaction (Boehringer, Mannheim, Germany).

2.4 | Immunohistochemistry

BEN, PAX6, and PAX7 immunohistochemistry was performed on floating vibratome sections according to Bardet et al. (2006). After several washes in PBT (0.1 M PBS with 0.5% Triton X-100; Sigma, St. Louis, MO, USA), the sections were treated with 3% hydrogen peroxide in PBT for 10 min in the dark to inactivate endogenous peroxidase activity. After two washes in PBT for 10 min each, sections were blocked in PBT-GA (PBT with 0.2% gelatin and 0.1% azide) and 0.1 M lysine (Sigma, Cat. No. L5626) during 90 min at room temperature. The primary mouse monoclonal antibody against chicken adhesion molecule BEN (SCI/DM-GRASP; DSHB Cat# BEN, RRID:AB_2313998), an IgG1 (a 95–110-kDa member of the immunoglobulin superfamily; Pourquié et al. 1990), was diluted 1:20 in PBT-GA and incubated overnight at 4°C. PAX7 monoclonal antibody was diluted 1:40 (DSHB Cat# pax7, RRID:AB_528428). After three washes in PBT (10 min each), sections were incubated with biotinylated goat anti-mouse IgG diluted in PBTG (1:200; Vector Laboratories Cat# BA-9200, RRID:AB_2336171) during 90 min. After three washes in PBT (10 min each), sections were incubated with avidin–biotin complex (1:330; Vector Laboratories Cat# PK-4000, RRID:AB_2336818) for 1 h. Next, sections were washed three times in PBT and two times in 0.05 M Tris–HCl (pH7.4), 10 min each. The reaction was developed for 15 min with 3,3-diaminobenzidine (1%; DAB; Sigma, St. Louis, MO, USA;) plus 0.03% hydrogen peroxide in 0.05 M Tris–HCl (pH7.4) during 4–15 min. The reaction was stopped with several washes in 0.05 M Tris–HCl. Finally, the sections were mounted, dehydrated, and then coverslipped with Eukitt (Fluka, Buchs, Switzerland).

The anti-BEN monoclonal antibody was raised against the chicken protein (Developmental Studies Hybridoma Bank). It was reported that this antibody recognizes cells that express the mRNA coding for the corresponding protein (Chédotal, Pourquié, and Sotelo 1995). The specificity of PAX7 antibody was demonstrated by Western blot studies and by comparison of the topographical localization of the immunoreaction with the mRNA expression pattern (Ferran et al. 2007).

2.5 | Imaging

Microscope slides carrying several reacted sections were scanned whole at high resolution using a digital scanner (ScanScope CS Aperio Technologies, USA; RRID:SCR_025111). ImageScope software (Aperio, RRID:SCR_020993) served to select and adjust in size and resolution the details of interest selected from the digital files. Further processing of the figures was carried out using Adobe Photoshop CS4 (RRID:SCR_014199) and Adobe Illustrator CS5 software (RRID:SCR_010279).

3 | Results

3.1 | Our Interpretive Model

Our analysis applies straightforwardly the anatomic and topologic assumptions of the updated prosomeric model (Figure 1a; Nieuwenhuys and Puelles 2016; Puelles, Martinez de la torre, Bardet et al. 2012; Puelles 2013, 2015, 2019; Puelles and Rubenstein 2015; Puelles 2013, 2016, 2018, 2019). The Dien-mesencephalic anatomic region covered is beset by numerous conceptual and terminological historical problems related to alternative definition of the brain axis, confused notions about the fundamental directions in morphologic space, discrepancies about various interregional boundaries, and controversial notions about partly unknown areas such as the prethalamus, the pretectum, the pre-isthmus, and the isthmus (reviews in Puelles 2016, 2019; Puelles and Hidalgo-Sánchez 2023). This is mostly due to unconciliable discrepancies between the classic columnar model of Herrick/Kuhlenbeck and the prosomeric model (see critical comparison in Figure 1a,b; see also Puelles and Rubenstein 1993, 2003, 2015, or Puelles 2018).

The relevant territories we need to contemplate are the Dien, the midbrain, and the rostral "prepontine" hindbrain (Puelles 2019; Watson, Shimogori, and Puelles 2017; Watson, Mitchelle, and Puelles 2017; Watson, Kirkcaldie, and Puelles 2017; Watson, Bartholomaeus, and Puelles 2019). In the updated prosomeric model, all three regions are proneuromeric units of the brain (Puelles 2018). The former two belong to the forebrain tagma, whereas the third enters the hindbrain tagma (Puelles 2018). The tagmatic character of the whole forebrain, including the added midbrain, is underpinned modernly by genoarchitectural similarities secondary to shared aspects of anteroposterior and dorsoventral molecular patterning. The whole brain, including forebrain and hindbrain, is divided into alar and basal longitudinal zones by a primary longitudinal boundary, the alar-basal limit (His 1893, 1895, 1904), which we now prefer to define molecularly (e.g., with *Shh* or *Nkx2.2* probes) rather than by the only tertiarily emergent morphogenetic phenomenon of the

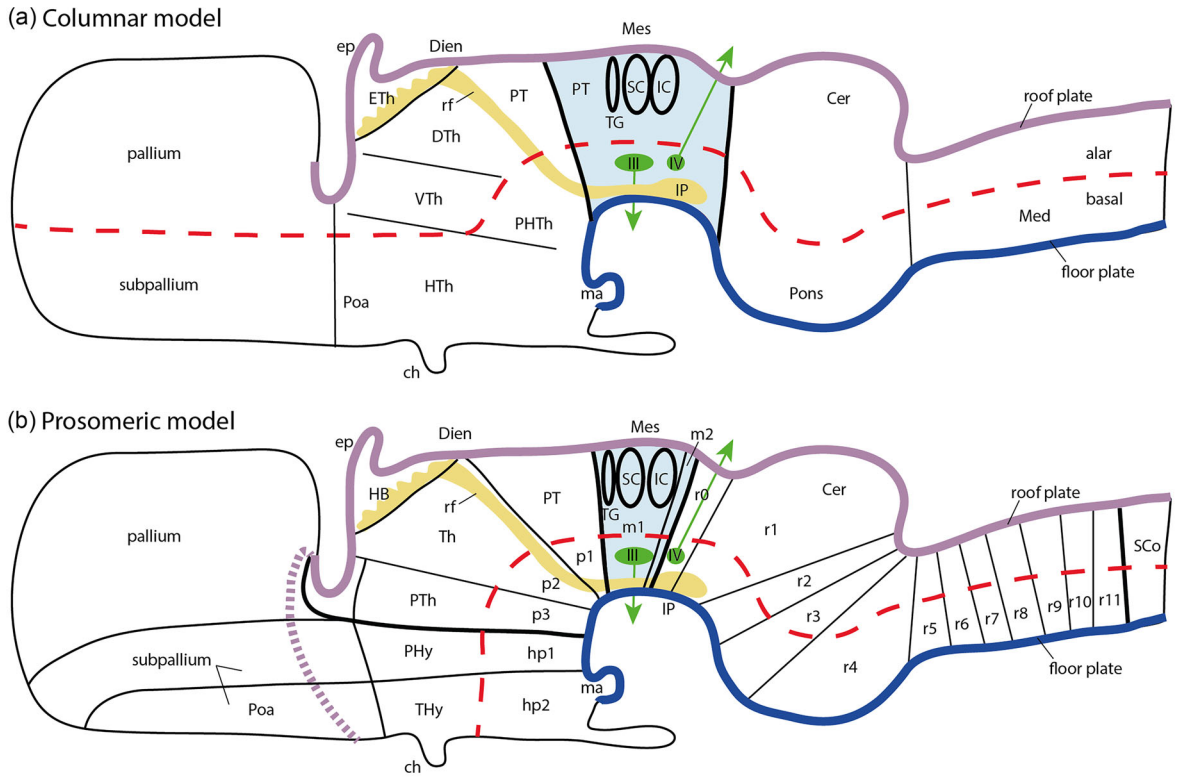

FIGURE 1 | Schemata illustrating differences in conceptual definition of diencephalic, midbrain, and rostral hindbrain brain regions between the columnar model (a) and the prosomeric model (b). Both schemata are made as similar as possible in order to emphasize the differences. The telencephalon appears at the left and the hindbrain at the right, dorsal being oriented upward. However, note the length axis postulated by the prosomeric model is represented here by the red dash line of the alar-basal boundary as identified molecularly, irrespective that such a subdivision is not accepted by the columnar model. (a) The classic columnar model indeed does not assume alar and basal plates in the forebrain and takes the forebrain axis to end in the telencephalon, separating there the pallium from the subpallium (some modern columnar model versions do accept the alar-basal boundary, though (see Swanson 2012). The dorsal and ventral thalamic plus hypothalamic columnar parts of the diencephalon (DTh, VTh, and HTh) are held to be limited by longitudinal ventricular sulci (gray lines), traced roughly parallel to the arbitrary axial reference (red dashes), but clearly orthogonal to the cephalic flexure marked by the bent floorplate (blue line) or to the roof plate midline (violet line). In this model, the midbrain (in blue background) is large and includes a caudal half of the PT and the prepontine or isthmic area caudally (thus encompassing both the oculomotor and trochlear cranial motor nuclei and nerves (III, IV; in green). The major midbrain analysis centers (tectal gray, superior and inferior colliculi, TG, SC, IC) lie intercalated in a central midbrain area. The interpeduncular nucleus, the target of the retroflex tract, is thus placed in the caudal midbrain (IP; retroflex fibers drawn in yellow, coming from the habenula or epithalamus, ETh). (b) The prosomeric model maintains instead that the alar-basal boundary (red dash line; a result of general dorsoventral patterning) courses essentially parallel to floorplate (blue line) and roof plate (violet line) through the forebrain, thus ending in the acroterminal surface of the HTh, ventrally to the optic chiasma (ch; note this leaves the eye as an alar entity, while it may be seen as basal in the other model). The whole prosomeric brain is thus divided into continuous alar and basal parts. Anteroposterior divisions of the forebrain include the hypothalamus-telencephalon complex or secondary prosencephalon, divided into two prosomeres (hp1, hp2; other abbreviations below), the diencephalon caudal to the hypothalamus (divided into diencephalic prosomeres p1-p3; note p1 includes here the whole pretectum, PT), and the midbrain (reduced to the basal III nucleus and nerve and the alar TG, SC, and IC centers). The midbrain is divided in two unequal mesomeres (m1 and m2) and limits caudally with the isthmus or rhombomere 0 of the prepontine hindbrain (there are 12 rhombomeres- r0-r11- before reaching the spinal cord; SC). It can be seen that, in general, prosomeric brain subdivisions are richer and more systematic and consequently allow more precise location of neural entities. Interestingly, the supposedly longitudinal diencephalic limits postulated by columnar authors (gray diencephalic sulcal lines in a) turn out to approximate transversal interneuromeric (intersegmental) boundaries in the prosomeric model (complete gray boundary lines orthogonal to roof, alar-basal boundary, and floor; the columnar dorsal and ventral thalami have become the thalamus and the prethalamus, Th, PTh). The spatial directions of such complete transversal limits seem to change because the axis of the brain is secondarily bent due to differential alar versus basal growth, but the interneuromeric limits are seen to be always orthogonal to the bent axial red-dash line. Moreover, the retroflex tract is noticed to course partly alongside the p1/p2 interneuromeric boundary, and the IV motor and the IP nuclei fall now in the rostral hindbrain. This rearrangement of boundaries is strongly supported by molecular and experimental evidence III, oculomotor nucleus and nerve; IV, trochlear nucleus and nerve; Cer, cerebellum; ch, optic chiasma; Dien, diencephalon; DTh, dorsal thalamus (columnar); ep, epiphysis; ETh, epithalamus (columnar); HB, habenula; hp1-2, hypothalamo-telencephalic prosomeres hp1 and hp2; HTh, hypothalamus (columnar); IC, inferior colliculus; IP, interpeduncular nucleus complex; m1-2, mesomeres m1 and m2; Med, medulla oblongata; Mes, mesencephalon; p1-3, diencephalic prosomeres p1-p3; PHTh, posterior hypothalamus (columnar); PHy, peduncular hypothalamus (prosomeric); Poa, preoptic area; PT, pretectum; PTh, prethalamus (prosomeric); r0-r11. rhombomeres r0 to r11; rf, retroflex tract; SC, superior colliculus; TG, midbrain tectal gray; Th, thalamus (prosomeric); THy, terminal hypothalamus (prosomeric); VTh, ventral thalamus (columnar).

classic sulcus limitans of His (Nieuwenhuys and Puelles 2016; Puelles 2013; Puelles and Rubenstein 2015; Puelles et al. 2013).

The forebrain accordingly ends caudally at the transverse mesrhombencephalic boundary (also known as the "isthmic boundary," though the isthmus proper is the rostralmost hindbrain prepontine neuromere (i.e., not a boundary); see Puelles 2013, 2018; Watson, Shimogori, and Puelles 2017). The ventromedian interpeduncular nucleus of the hindbrain tagma lies entirely caudal to this limit but is stretched over three rhombomeres (see below). It is, accordingly, strictly *a plurineuromeric prepontine hindbrain structure* (Figure 1b). In contrast, literature based on the columnar model uniformly ascribes the interpeduncular nucleus to the "midbrain" (when not to the Dien), apparently because this now outdated model disregards the relevant transverse midbrain limits that converge into the cephalic flexure (cf) rostral and caudal to the oculomotor nerve root, first described by Palmgren (1921) (III; Figure 1a; see also Puelles 2019; Vaage 1969, 1973).

The diencephalic proneuromere is secondarily divided rostrocaudally into three diencephalic prosomeres identified as dp1-dp3, or simply p1-p3, ordered caudo-rostrally (Figure 1b). Their alar domains are known modernly (under prosomeric assumptions) as pretectum (p1), thalamus (p2), and prethalamus (p3). Their basal domains constitute the tripartite diencephalic tegmentum, where longitudinal fibers predominate (Diaz et al. 1999). This basal zone is continuous with the mesencephalic tegmental counterpart and jointly displays the mesodiencephalic substantia nigra/ventral tegmental area dopaminergic complex (Puelles and Medina 1994). In the prosomeric model (Figure 1b), the classic epithalamus or habenular region is included in the thalamus (alar p2), wherein it forms a hyperdorsal (roof-adjacent) *habenular progenitor area* with distinct molecular and connective properties (Figure 2c). In its turn, the midbrain proneuromere is divided into two midbrain prosomeres, known as "mesomeres" 1 and 2 (m1, m2; Figure 1b; Hidalgo-Sánchez et al. 2005; Palmgren 1921; Puelles 2018; Puelles and Hidalgo-Sánchez 2023; Puelles and Martinez-de-la-Torre 1987; Vaage 1969, 1973).

As regards the hindbrain, we are interested only in its rostral prepontine proneuromere because it contains the interpeduncular nucleus (this rostral hindbrain region was classically wrongly ascribed to the midbrain; compare Figure 1a,b; see also Puelles 2016, 2019). It results are divided into two classic "rhombomeres": the isthmus (or r0) and rhombomere r1 (Palmgren 1921; Puelles 2018; Vaage 1969, 1973). However, r1 is double as large as a standard rhombomere, and eventually it subdivides (both molecularly and as regards differential structural nuclear fates) into rostral and caudal neuromeric moieties called rostral and caudal r1 (r1r, r1c; Alonso et al. 2012; Lorente-Cánovas et al. 2012; Moreno-Bravo et al. 2014; Vaage 1969, 1973). The prepontine hindbrain proneuromere accordingly is tripartite (r0, r1r, and r1c). This is where the *plurineuromeric interpeduncular nuclear complex* forms after a complex set of tangential and radial migrations studied by Lorente-Cánovas et al. (2012) (see also García-Guillén et al. 2020, 2021; Moreno-Bravo et al. 2014).

All interneuromeric boundaries are by definition topologically transversal, irrespective that the axial bending of the neural tube at the cf alters their apparent topography (cf; Figure 1b; note the axial bending is caused by disproportionate surface growth of the alar domains relative to the less dynamic basal domains).

In all vertebrates, the retroflex tract forms at the caudal aspect of the thalamus, under the habenular region (lateral and medial habenular nuclei), where its fibers originate. Fibers coming from the rostral parts of the HB first circulate caudalwards in a horizontal subhabenular interstice formed between the main thalamic mass and the overlying HB (i.e., the habenular efferent fibers normally clearly eschew penetrating the thalamus already at the initial stages of their growth). All efferent habenular components thus collect caudally, under the thalamic retrohabenular area, and in front of the dorsal pretectum. The tract next turns ventralwards in right angle and proceeds in a straight dorsoventral course along the caudalmost part of the thalamic alar and basal plates (p2; Figure 1b). This represents within the prosomeric model a topologically *transversal* dorsoventral route just in front of the thalamo-pretectal interneuromeric boundary (Figure 1b; see also our mouse data in Figure 2a,b,e). Once they are close to the thalamic FP, the fibers bend ipsilaterally backwards at 90°; this is the retroflexion originally observed by Meynert (1872). Thereafter, the fibers progress longitudinally in a paramedian position through the pretectal (p1) and midbrain (m1 and m2) tegmentums until they reach terminal distribution within the interpeduncular nuclear complex in the prepontine hindbrain (r0, r1r, and r1c).

Earlier studies based on the columnar model of Herrick (1910, 1948) did not precisely define the location of the retrothalamic dorsoventral course nor identify the latter as topologically transversal because all transverse interneuromeric borders (including the thalamo-pretectal boundary) were disregarded in that model, emphasizing instead hypothetic longitudinal columns (Figure 1a). The rostral pretectum was partly ascribed to the habenular epithalamic longitudinal column and partly to the underlying longitudinal dorsal thalamus column; moreover, the caudal pretectum was visualized as lying within the rostral midbrain (compare Figure 1a,b). After its retroflexion, the subsequent longitudinal ventral paramedian course of the retroflex tract into the hindbrain was also not defined precisely in studies based on the columnar model because the latter misplaces the interpeduncular nucleus as lying *inside* the midbrain tegmentum (Figure 1a). Rather than a retroflexed course (as shown realistically in Figure 1b, compare Figure 2a), many published columnar schemata depict a *straight* retroflex tract extending obliquely from the HB into the interpeduncular nucleus. The general columnar notion was accordingly that the tract originates in the dorsal habenular area and approaches *obliquely* or *directly* in a straight course the ventral interpeduncular complex, imagined to lie within the basal midbrain or even in the caudal Dien (this false notion is still found in some present-day literature, thus justifying the present clarifying comments; e.g., Bayer and Altman 2004; Paxinos et al. 2023; Swanson 1998, 2012).

In Figure 2, we compare mouse and chick mid-embryonic preparates at E16.5 and stage HH36, respectively, using ISH for *Tcf7l2* (chicken stage HH36 corresponds to 10 days in ovo; Lee et al. 2017). The expression of this marker labels the alar plate mantle territories of thalamus, pretectum, and midbrain, whereas the signal is weak or absent at the habenular nuclei, as well as in

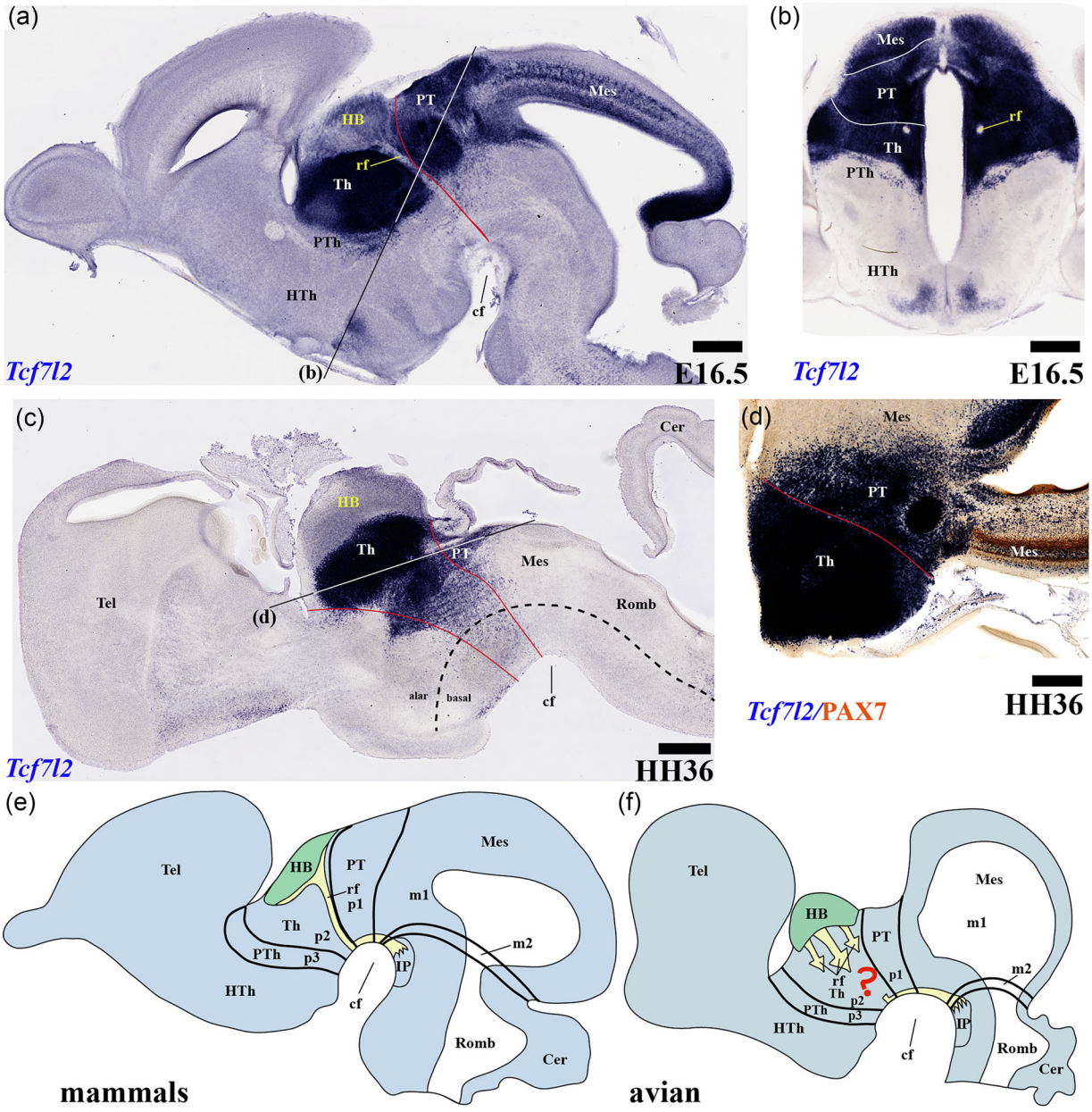

FIGURE 2 | Plate illustrating the different visibility of the retroflex tract in the mouse (a and b) and the chick (c and d). Schemata are added indicating what we know or don't know initially about the respective situations (e and f). The cephalic axial flexure referred to in Figure 1 is marked in (a, c, e, f) cephalic flexure (cf). (a and b) Sagittal and horizontal sections through E16.5 mouse embryos reacted for *mTcf7l2* ISH (blue signal; the horizontal section plane is marked as a white/black straight line in (a) (note it also interests a distant hypothalamic gene signal; HTh). This gene typically is expressed in the thalamus (Th; alar p2), the pretectum (PT; alar p1), and part of the midbrain tectal plate (Mes); there is weak partial expression in the habenular area (HB). The retroflex tract (rf) is visible in both sections as a compact negative periventricular fiber packet running dorsoventrally between Th and PT (white lines in b mark the corresponding transverse boundaries). (c and d) These sagittal and horizontal diencephalic sections in the chick (horizontal section plane indicated by white line in (c) were reacted for *cTcf7l2* ISH at 10 days of incubation (stage HH36; blue signal) showing similar distribution in Th, PT, and Mes and light signal in HB, as in the mouse, but no retroflex tract whatsoever is visible. The section in (d) also immunoreacted for PAX7 protein (brown signal). (e and f) These schemata point out that while the whole course of the retroflex is visible and well known in mammals such as the mouse (e), only the beginning and the end of such a course are known in the chick (f). This raises the question of how the avian retroflex fibers reach their target.

the Dien-mesencephalic basal plate or tegmentum (Figure 2a–d; Lee et al. 2017). In the mouse, the characteristic *Tcf7l2*-negative retroflex bundle (rf) appears just in front of the thalamo-pretectal boundary (red line; Figure 2a,b,e) in both sagittal and horizontal sections (the horizontal section plane is indicated in Figure 2a). Instead, comparable chicken sagittal and horizontal sections do not show any retroflex tract bundle (Figure 2c,d,f).

The diagram in Figure 2e depicts the full course of the mouse retroflex tract into the hindbrain interpeduncular complex. The

diagram in Figure 2f suggests that the retroflex tract must exist in birds as it apparently originates in the HB and reaches finally the homologous interpeduncular complex (see Section 1), but the course of its fibers between the HB and the paramedian hindbrain basal plate needs to be determined (question mark). We approached this issue by performing mappings of BEN protein at stages HH30 and HH35 (6.5 and 9 days in ovo). We followed in this approach the work of Chédotal, Pourquié, and Sotelo (1995), who showed at early embryonic stages that this antibody labels specifically the diencephalic habenular efferent fibers in the chick (apart other elements elsewhere).

3.2 | BEN Observations at HH30

We show first representative sagittal sections through the chicken Dien at HH30 (6.5 days in ovo), cut through the thalamus at medial, intermediate, and lateral parasagittal levels (Figure 3a–h). These sections were first reacted for *FoxP2* ISH (blue signal), and alternate sections were immunoreacted afterward for BEN (brown color; protocol of Ferran et al. 2015b; in our hands, previous ISH treatment enhances the intensity and selectivity of the BEN immunoreaction). The *FoxP2* ISH reaction conveniently provides labeling of the relevant prethalamic, thalamic/habenular, and pretectal background and aids the identification of the related interprosomeric boundaries (e.g., the zona limitans [ZLI], or zli, between prethalamus and thalamus, or the thalamo-pretectal boundary). In some sections (Figures 3c,d,f,g and 4d,e) there appears as well the subthalamic nucleus (STh), a caudal hypothalamic tegmental landmark placed rostral to the prethalamic tegmentum (Jiao et al. 2000; Puelles, Martinez-de-la-Torre, Bardet, et al. 2012).

The BEN-labeled retroflex tract fibers are best seen in the medialmost section shown (Figure 3a), which confirms a similar deep periventricular position of the tract as is found in the mouse (Figure 2b) and other vertebrates. Efferent retroflex tract fibers originate abundantly throughout the longitudinal extent of the habenular area (Hab; Figure 3a). We readily notice that most chicken habenular efferents do not collect first under the caudal HB following a longitudinal caudally directed subhabenular course, which would eschew entering the underlying thalamus. Instead, most of the fibers penetrate orthogonally the habenulo-thalamic boundary and course in a defasciculated parasagittal fan-like pattern through the thalamus, with different axonal bundles approaching gradually the ZLI (Figure 3a; the p3/p2 limit) or the local alar-basal boundary (Figure 3a). A significant number of fibers actually cross the ZLI, thus entering the alar prethalamus (PThal; p3). Here, they immediately turn ventralwards in a transversal dorsoventral course toward the prethalamic basal plate, keeping close to the ZLI (Figure 3a–d,g,h). At the caudal end of the HB, we see a number of efferent habenular fibers that penetrate minimally the thalamic main mass and perhaps even the pretectum (Figure 3a,b), and thus course ventralwards approximately along the standard retrothalamic trajectory in front of the thalamo-pretectal boundary (p2/p1 limit), thus normally reaching the thalamic tegmentum (Figure 3a–d; fibers that possibly have invaded the pretectum may be seen coursing dorsoventrally through the precommissural pretectum in Figure 3d). There are also some other fibers that follow intermediate transthalamic courses into the underlying tegmentum (Figure 3a–c), so that the roughly dorsoventrally coursing habenular efferents are spread across most of the alar thalamic mass and corresponding tegmentum rather than concentrating caudally next to the pretectum. A few retroflex tract fibers seem to cross obliquely the thalamo-pretectal limit and course dorsoventrally within the rostral pretectal tegmentum (Figure 3a,b).

If we examine now more lateral sagittal sections from the same HH30 specimen, we observe that the atypical transthalamic habenular fibers can be observed practically at all levels (Figure 3b–d,g,h). Some atypical transthalamic fibers cross the ZLI even at very superficial parasagittal section levels (e.g., Figure 3h). This result indicates that, as they cross the thalamus, the transthalamic fibers are also partly dispersed in the radial dimension (i.e., the ventriculo-pial dimension) and thus occupy a sizeable part of the main thalamic cell mass, with apparent exception of the extreme periventricular and subpial strata (Figure 3a–d).

3.3 | Observations at HH35

Entirely comparable observations were obtained in our sagittally sectioned HH35 material (Figure 4a–f). Both thalamus and prethalamus appear now more developed, having grown dorsoventrally. There are indications of incipient subdivision of the main thalamic mass into the dorsal, Intermediate, and ventral pronuclei or *thalamic tiers* described previously by our group (Thal; dt; it; vt; Figure 4a,b; see Diaz, Yanes et al. 1994; Dávila et al. 2000; González, Puelles, and Medina 2002; Martínez-de-la-Torre et al. 2002; Puelles 2001; Puelles et al. 2007, 2019; Redies, Arndt, and Ast 2000; Yoon, Puelles, and Redies 2000). Atypically coursing efferent habenular fibers are seen at the three indicated tiers of the thalamus (Figure 4a–c). As observed in the HH30 specimen, the caudalmost habenular efferent fibers passing next to the molecularly distinct retrohabenular thalamic area (asterisk in Figure 4d–f) form a slightly denser packet that thereafter courses dorsoventrally in front of the thalamo-pretectal boundary (Figure 4a–c). These fibers are just one end of the fan-shaped large bundle that permeates all the thalamic mass, whose elements variously course obliquely and dispersedly through the main thalamic cell mass, as can be clearly appreciated in coronal sections (see Figures 5a–i and 6a–f). As observed in sagittal sections, the atypical fibers invade the thalamic mantle preferentially through the intermediate thalamic tier (which contains the primordia of the collothalamic rotundus and triangular nuclei; Huber and Crosby 1929; Martínez-de-la-Torre et al. 2002; Puelles 2001). More dispersed fibers penetrate the dorsal thalamic tier (primordium of the main visual and somatosensory thalamo-telencephalic relay centers; Figure 4a–c). The ventral thalamic tier (which contains periventricularly the primordium of the avian medial geniculate homolog, the classic ovoidal nucleus; see Puelles et al. 2007, 2019) contains few if any fibers oriented rostralwards, showing predominantly dorsoventral courses of transthalamic fibers partly deflected from the standard caudal tract (Figure 4a–c).

Figure 4d–f illustrates molecular evidence allowing our tracing of neuromeric boundaries (red lines) in HH35 chick embryo specimens unreacted with the anti-BEN antibody but hybridized in situ for *Pax6* (note they are also immunoreacted with PAX7

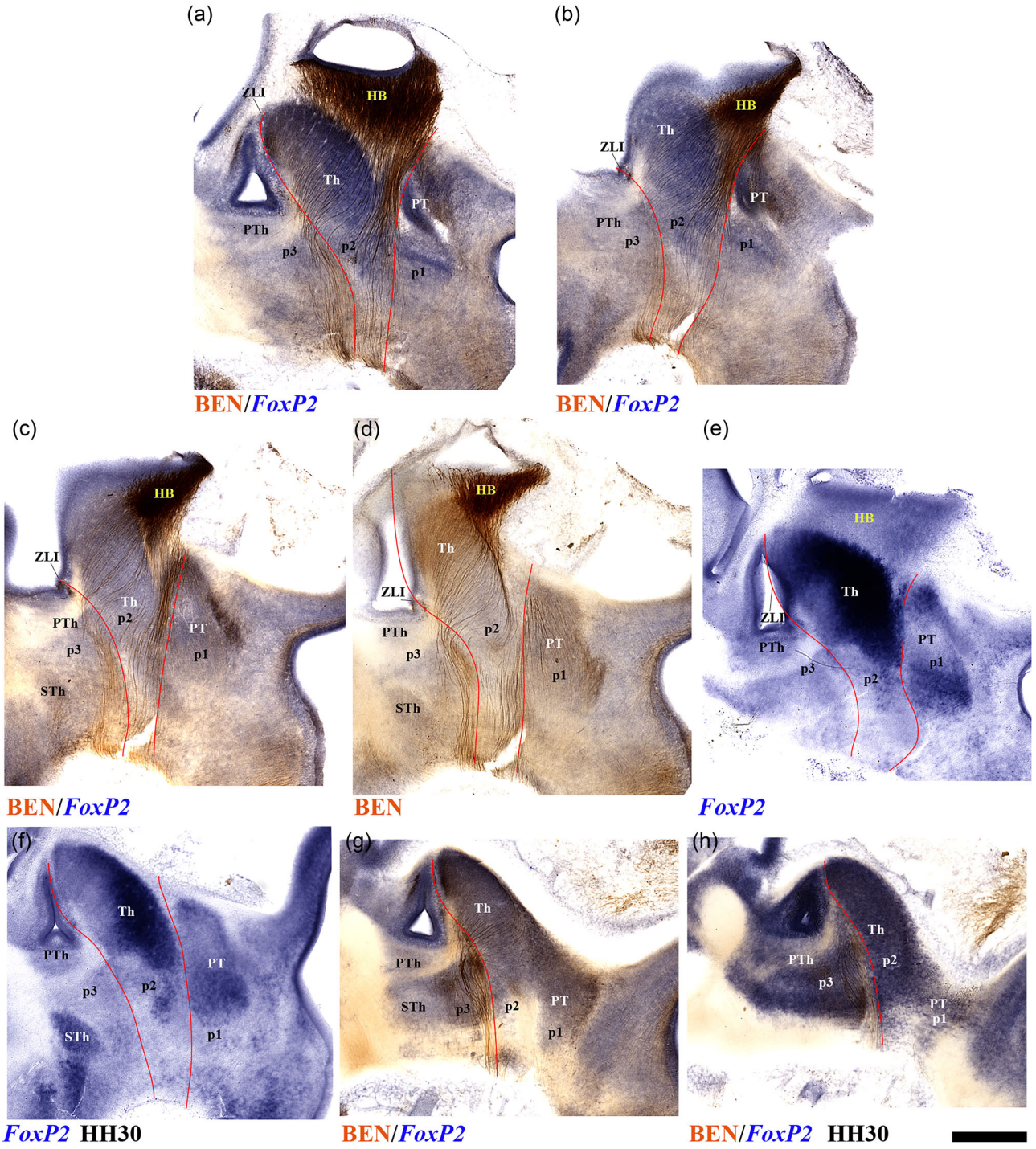

FIGURE 3 | Plate showing sagittal sections through the chick diencephalon at stage HH30, ISH-reacted for *FoxP2* (blue signal) and immunoreacted for BEN protein (brown reaction). Though the different sagittal sections come from different specimens, they are roughly ordered from medial to lateral. Rostral lies to the left and ventral at the bottom. (a and b) These are the medialmost sections passing through periventricular levels where the retroflex tract would be expected to be seen if its course was standard (i.e., similar to the mammalian one). The habenular region (Hab) appears well developed and shows many labeled efferent fibers oriented dorsoventrally. The caudalmost stained fibers collect into a positionally standard retrothalamic retroflex tract component, just in front of the pretecto-thalamic boundary (red line between Th and PT); some of these retroflex fibers reach vertically the underlying thalamic tegmentum. More rostral habenular fibers, however, do not course backwards in the subhabenular area and instead enter vertically the ovoid thalamic mass (compare the background *Foxp2* thalamus labeling with the exclusively ISH-reacted specimens in e and f). These fibers can be seen crossing the thalamic mass more or less obliquely, so that some of them come to cross rostralwards the zona limitans interthalamic boundary (red line separating PTh/p3 from Th/p2). In a, the fibers entering the prethalamus are seen bending ventralwards into the tegmentum closely in front of the interthalamic boundary. Similar prethalamic coursing fibers are seen in slightly more lateral parasagittal sections (c and d) or in far lateral sections (g and h).

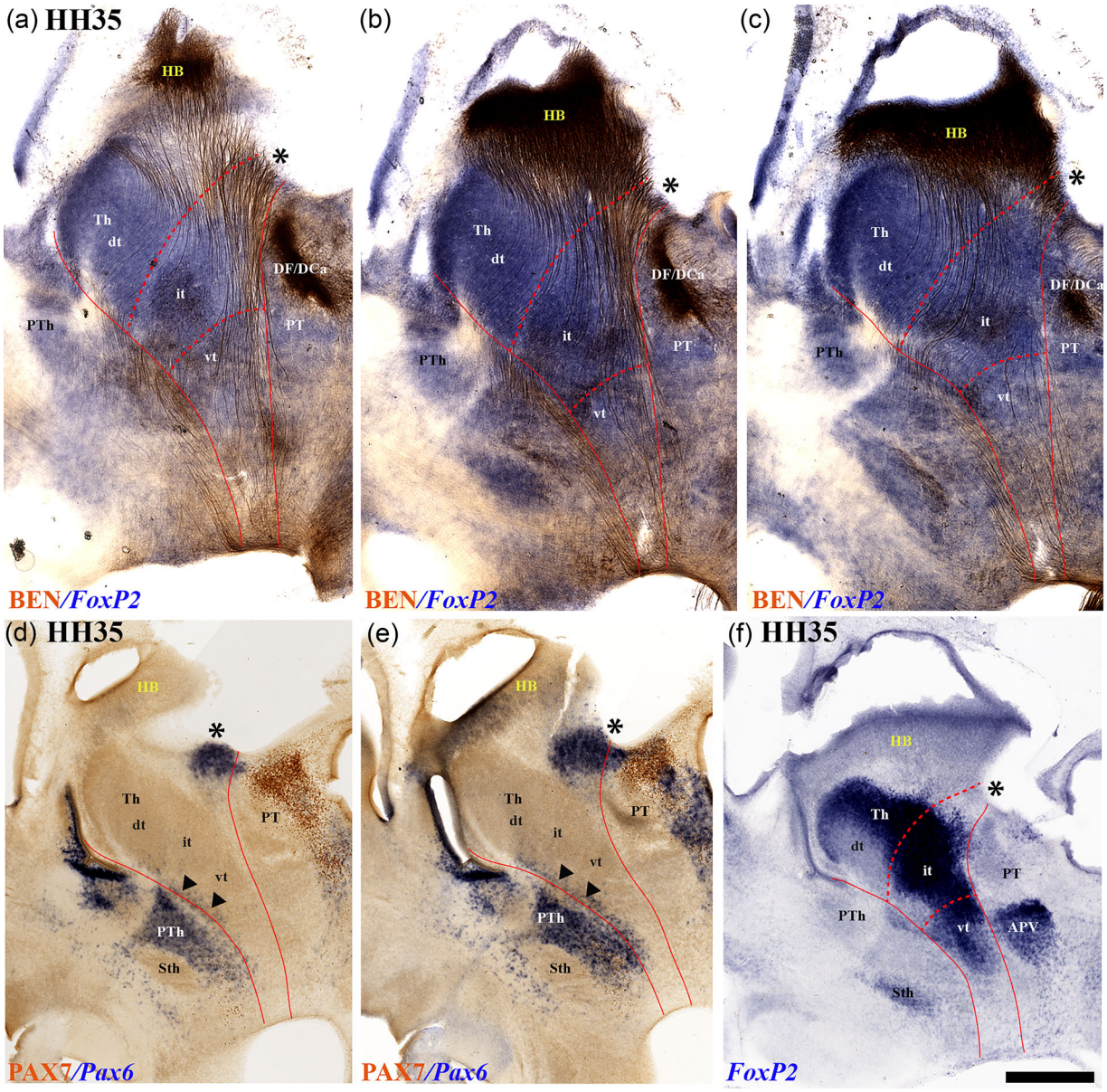

FIGURE 4 | Plate showing sagittal sections (a–f) through the chick diencephalon at stage HH35, ISH-reacted for *FoxP2, Meis1*, or *Pax6* (blue signal; indicated at bottom) and immunoreacted for BEN and PAX7protein (brown reaction). Though the different sagittal sections come from different specimens, they are roughly ordered from medial to lateral. In the sagittal sections rostral lies to the left and ventral at the bottom. At the top, we see the pretecto-mesencephalic transition. Continuous red lines mark the interneuromeric boundaries separating prethalamus (PTh) from thalamus (Th) and pretectum (PT). Red dash lines in (a–c) and (f) label the longitudinal limits of the dorsal, intermediate, and ventral pronuclear tiers of the thalamus (dorsal tier [dt], it, vt). The asterisks in (a–c) indicate the area where a mass of retrohabenular **Pax6**-expressing thalamic neurons is found (compare ISH reaction and asterisk in (d and e). (a–c) These medial sagittal sections show the brown fibers coming out of the habenular area (HB). As in Figure 3, the caudalmost retroflex fibers course in retrothalamic position dorsoventrally in front of the pretectum. Some fibers can be seen reaching the p2 tegmentum. Other more rostral habenular fibers enter the thalamic mass and cross it obliquely, so that some reach the underlying p2 tegmentum and others the alar prethalamus, wherein they course into the p3 tegmentum (PTh; a–c; compare in d, e selective *Pax6*-labeling of various prethalamic cell masses, as well as a thin band of *Pax6*-positive cells just behind the interthalamic boundary (posterior shell of the zona limitans (black arrowheads). Note also the *Pax6*-negative subthalamic nucleus (Sth), identifying a basal component of the peduncular hypothalamus, which also expresses *FoxP2* (Figure 4f). PAX7 identifies pretectal commissural derivatives (Figure 4d,e).

antibody; Figure 4d,e) or for *FoxP2* (Figure 4f). *Pax6* ISH expression typically identifies some alar prethalamic cell populations (lying caudal to the *Pax6*-negative but *Foxp2*-positive hypothalamic STh; Figure 4d–f). *Pax6* reaction also underlines the thalamic shell subregion of the ZLI, which identifies the interprosomeric dp3/dp2 boundary (black arrowheads; red line), as well as a restricted dorsal *Pax6*-positive retrohabenular area (mentioned above) within the subpial intermediate thalamic tier that is traversed by many BEN-labeled habenular fibers (locus marked with asterisk; Figure 4a–e); this retrohabenular area is devoid of *FoxP2* expression (Figure 4f) and corresponds to the singular caudal retrohabenular thalamic locus where the whole retroflex

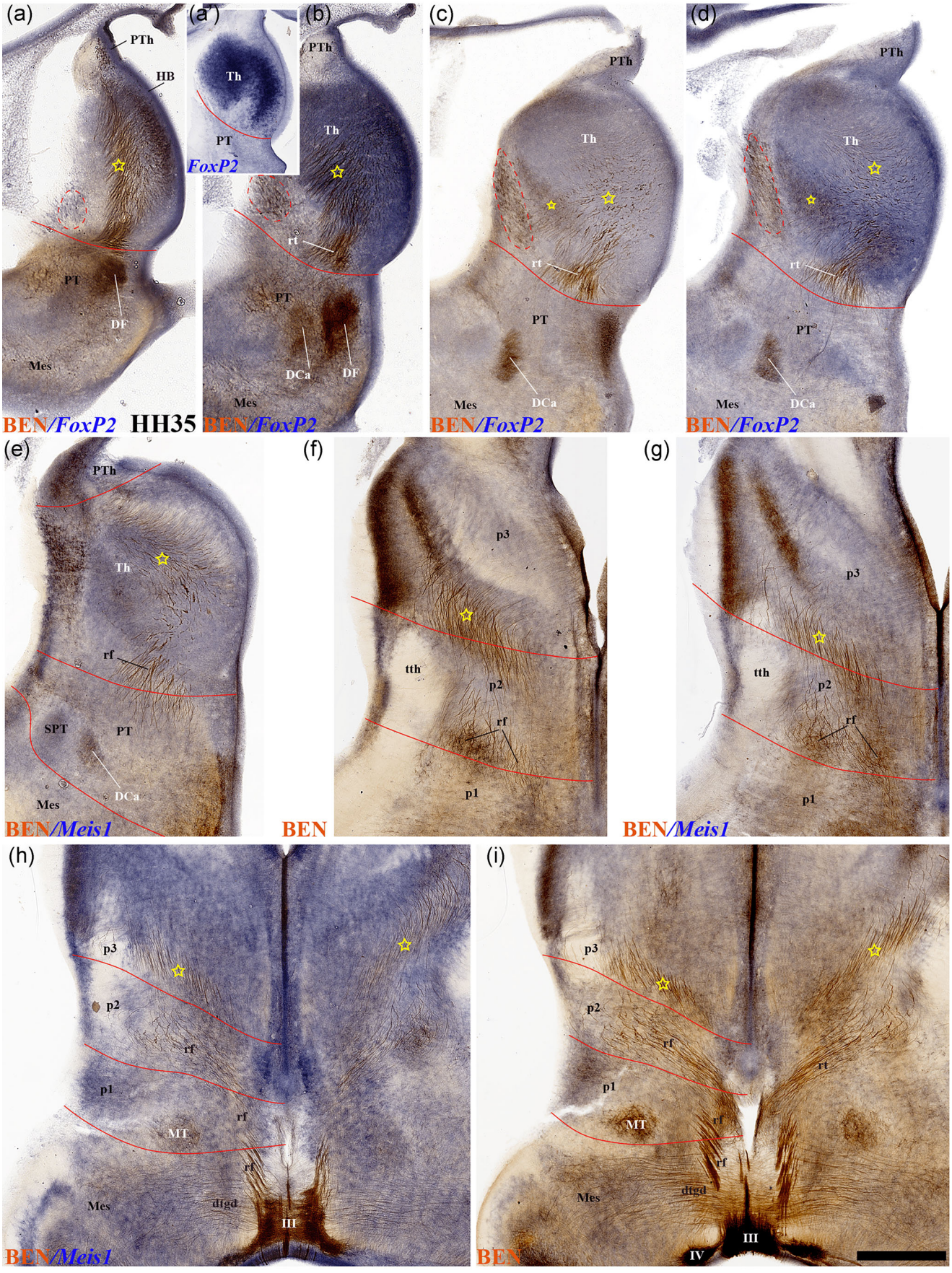

FIGURE 5 | Legend on next page.

tract normally collects in other vertebrates. Caudally within the pretectum, the commissural pretectal subdomain containing the posterior commissure is also typically *Pax6* and PAX7 positive (see Figure 4d,e).

An alternative view of the course of the standard and atypical chick habenular efferents is provided by serial coronal sections, likewise at stage HH35 (Figures 5a–i and 6a–f). The rostrally directed transthalamic fibers crossing the intermediate and dorsal thalamic tiers (asterisk in Figure 5a–e) pass into the alar prethalamus through the ZLI (p3/p2) limit (asterisk in Figure 5f) and thereafter course ventralwards within the prethalamus into the underlying prethalamic tegmentum (Figure 5g–i). At stage HH35, our coronal-sectioned material does not show clearly the interpeduncular nucleus, and the tightly aggregated radial glia fibers of the midbrain and hindbrain FP also stain strongly with the anti-BEN antibody, as does likewise the roof plate (FP; Figure 6a–f). Once the retroflex tract approaches the hindbrain locus of the interpeduncular nucleus complex (IP) complex, its right and left sections seem to grow for a while in surface while losing the contrast between individual fibers, suggesting possible entrance into a retroflex terminal field (rtf; Figure 6c–f). However, the rtf formations are bilateral and are not seen to send zigzaging fibers across the midline, perhaps obscured by the stained FP. A comparative schema of the present results on the course of the retroflex tract in the mouse and chick is presented in Figure 7a–d.

4 | Discussion

The habenulo-interpeduncular or retroflex tract is normally readily visible in mammals as a compact, well-localized bundle with a stereotyped course (e.g., Puelles, Watson et al. 2012; Puelles, Martinez-de-la-Torre et al. 2012; our Figure 1a,b) and reptiles (e.g., Beccari 1943; Diaz and Puelles 1992; Nieuwenhuys, ten Donkelaar, and Nicholson 1998), but is not distinct in birds (mentioned but not shown in Kuhlenbeck 1977, p.290; it was only tentatively identified in the chick stereotaxic atlas, plate 76 of Puelles et al. 2007, 2019; and Ferran et al. 2009). The cholinergic medial habenular fibers demonstrated photographically in the pigeon by Medina and Reiner (1994) in coronal sections do not allow to assess whether they are in strict topographic correlation with the thalamo-pretectal boundary (thus following a standard course); the authors do not illustrate these fibers in sagittal sections; they nevertheless appear in the first three diagrams of their Figure 6 (mapping oblique coronal sections), where they lie in the midst of the thalamus and are seen crossing the subrotundus nucleus that lies alongside the ZLI, and passing into the prethalamus, where they apparently collect into the subsequent tegmental caudopetal course. The authors do not comment on their implicitly abnormal course. As regards anamniotes, the retroflex tract is well documented in the lamprey and hagfish (Nieuwenhuys, ten Donkelaar, and Nicholson 1998, vol.1; Pombal and Puelles 1999), as well as in cartilaginous and teleost fishes (Nieuwenhuys, ten Donkelaar, and Nicholson 1998, vol.2), salamanders, and tritons (Herrick 1948; Puelles 2021). In contrast, this tract is not easily visualized in the frog brain when using standard myelin stains or immunoreaction for calcium-binding proteins (Beccari 1943; Kappers, Huber, and Crosby 1936; Kemali and Braitenberg 1969; Milan and Puelles 2000), but has been clearly identified with axonal tracing methods (Kemali and Lázár 1985; Kemali et al. 1980; Kemali and Guglielmotti 1982), as well as with AChE histochemistry (Puelles, Milán, and Martínez-de-la-Torre 1996). The latter study found a tract course fragmented into several fiber packets descending dorsoventrally separately through the frog thalamus, which later reaggregated as they advanced rostrocaudally through the underlying tegmentum into the interpeduncular nucleus.

On the whole, our data on the retroflex tract confirm its constancy in the diverse vertebrate lineages, though we point out occasional transthalamic variation of its course, as seen modestly in frogs and more markedly in the chick (or birds in general). Our BEN immunoreactions in chick embryos at 6.5 and 9 days of incubation (later stages than the early embryonic results of Chédotal, Pourquié, and Sotelo 1995) show that a positionally standard (retrothalamic) retroflex tract component exists that reaches normally its final interpeduncular target at the isthmus and rhombomere 1. This is the "lateral" component described in the dove by Huber and Crosby (1929). In any case, even this "standard course" component also seems to be sufficiently dispersed that a compact fiber packet is not visible at stage HH36 or later (Figure 2c,d). This dispersion is what causes the remarkable invisibility of the tract, as we demonstrated comparing chick and mouse material sectioned sagittally and horizontally and reacted by ISH for the ortholog *Tcf7l2* gene marker, a general label in this case for thalamic and pretectal neurons. Other atypical avian retroflex tract components show instead a widely dispersed intermediate transthalamic course (the "medial" component of

FIGURE 5 | (a and b) These coronal sections (*FoxP2* counterstained) at HH35 show dorsally just under the habenula the whole packet of efferent retroflex tract fibers, disposed in a more compact standard-like caudal part (rt) in front of the pretecto-thalamic border (red line) and extending rostralwards into more dispersed and rostral atypical part crossing the thalamus mainly through its intermediate stratum (large yellow asterisk). Less dense fibers also course more deeply and more superficially. The subpial marginal stratum seems devoid of retroflex fibers, though other BEN-positive fibers can be seen there, possibly belonging to the developing optic tract (areas surrounded by red dashes in (a and b). Inset A' shows only a *FoxP2* reacted adjacent dorsal coronal section through the thalamus, wherein the intermediate stratum apparently occupied by standard retroflex fibers appears as a caudal locus partly devoid of *FoxP2* signal. Sections (c and d) demonstrate slightly more ventral section levels through the thalamus (counterstained with *Foxp2*) illustrating packets of atypical transthalamic fibers marked with a large yellow asterisk (a small yellow asterisk marks a relatively superficial packet of atypical transthalamic fibers under the optic tract -red dash line). (e). *Meis1*-labelled coronal section showing the approach of transthalamic habenular fibers (large yellow asterisk) to the interthalamic zona limitans (red line). (f and g) Two more ventral coronal sections taken at levels where a significant packet of atypical transthalamic fibers have crossed already the ZLI into the alar prethalamus and now course dorsoventrally into the corresponding tegmentum (large yellow asterisk). The standard retroflex tract remains separately visible (rt). (h and i) Both standard retrothalamic (rt) and atypical prethalamic fibers (large yellow asterisk) course separately dorsoventrally within p2 and p3, respectively, into the tegmentum, previous to bending caudalwards therein. Some retroflexed rt fibers have continued their course into the neighborhood of the oculomotor midbrain nucleus.

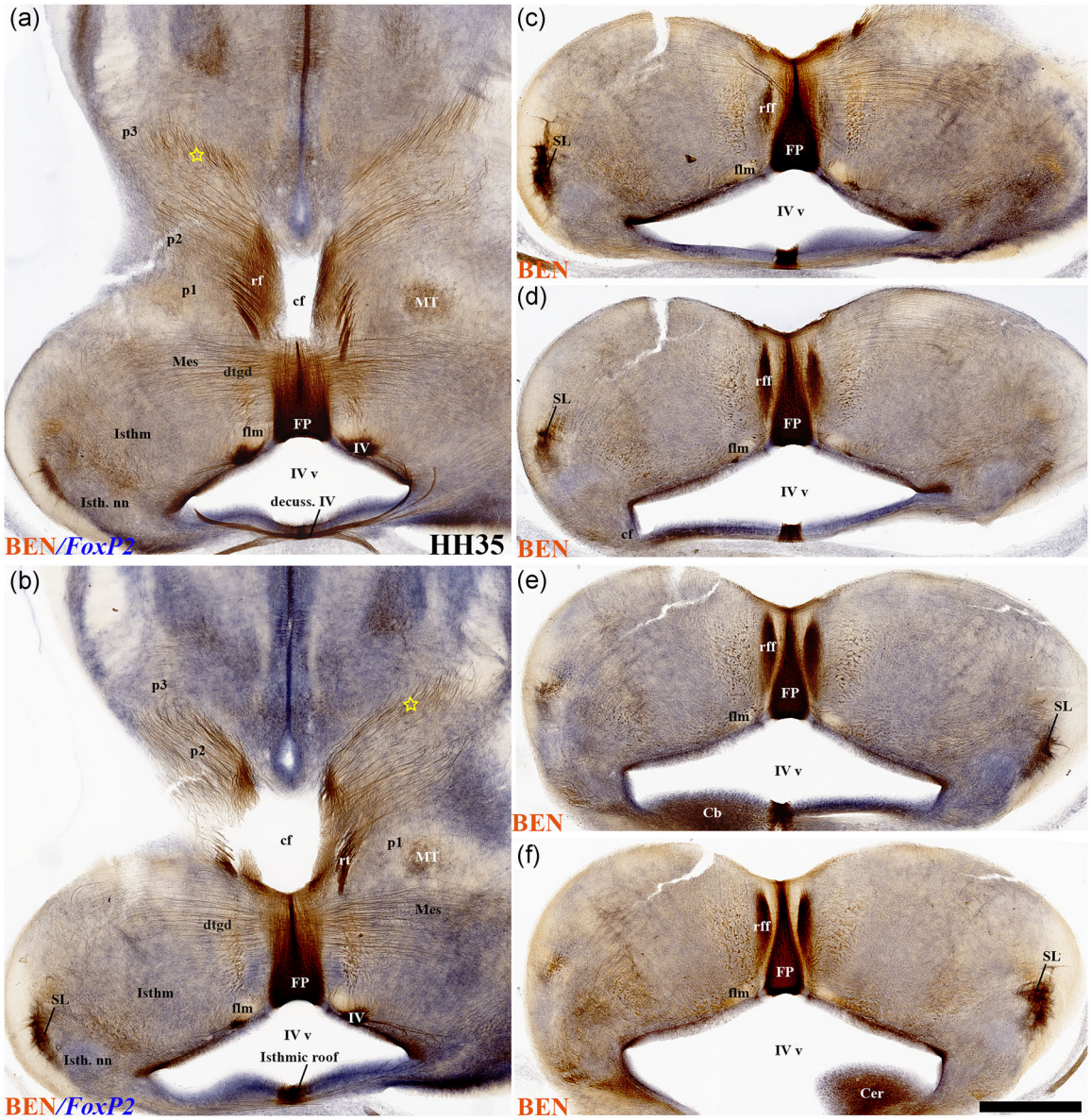

FIGURE 6 | (a and b) These coronal section levels at HH35 intersect the cephalic flexure (cf) under the pretectal and oculomotor midbrain region, at levels through the dorsal tegmental decussation of the midbrain (dtgd) and the isthmic trochlear nucleus (IV). They show progressive paramedian aggregation of transprethalamic (large yellow asterisk) plus transthalamic and standard retroflex fiber packets (rt) in the pretectal and midbrain tegmentum as they proceed caudalwards subsequent to their retroflexion. (c–f) More caudal section levels illustrate the joint entrance of the habenular efferents into the hindbrain isthmus and rhombomere 1 levels where the median primordium of the interpeduncular nucleus complex is forming.

Huber and Crosby 1929) that even brings some rostrally oriented atypical fibers to exit the thalamus across the ZLI, reaching the prethalamus. There they immediately descend dorsoventrally into the correlative tegmentum, coursing throughout in front of the ZLI interthalamic boundary (Figure 7c,d). Other fiber packets adopt intermediate-atypical courses. The diverse transthalamic fiber packets observed eventually all perform individual retroflexions similar to the standard case in the neighborhood of the diencephalic FP, previous to joining finally the descending common longitudinal tegmental course of the "standard" elements of the tract, thus reaching together the hindbrain IP. We did not observe retroflex fibers entering the hypothalamus (HTh).

4.1 | Parts of the Retroflex Tract Course

We suggest that the standard course of the retroflex tract observed in mammals and most vertebrates consists of four parts (color-coded in Figure 7a,b):

1. *Subhabenular course*: This is the initial normal longitudinal caudalwards course under the habenular nuclei and the thalamic retrohabenular area, by which the individual rostrocaudal habenular efferents normally collect into a single longitudinal tract.
2. *Retrothalamic course*: This is the subsequent normal dorsoventral course across the thalamic alar plate in front of

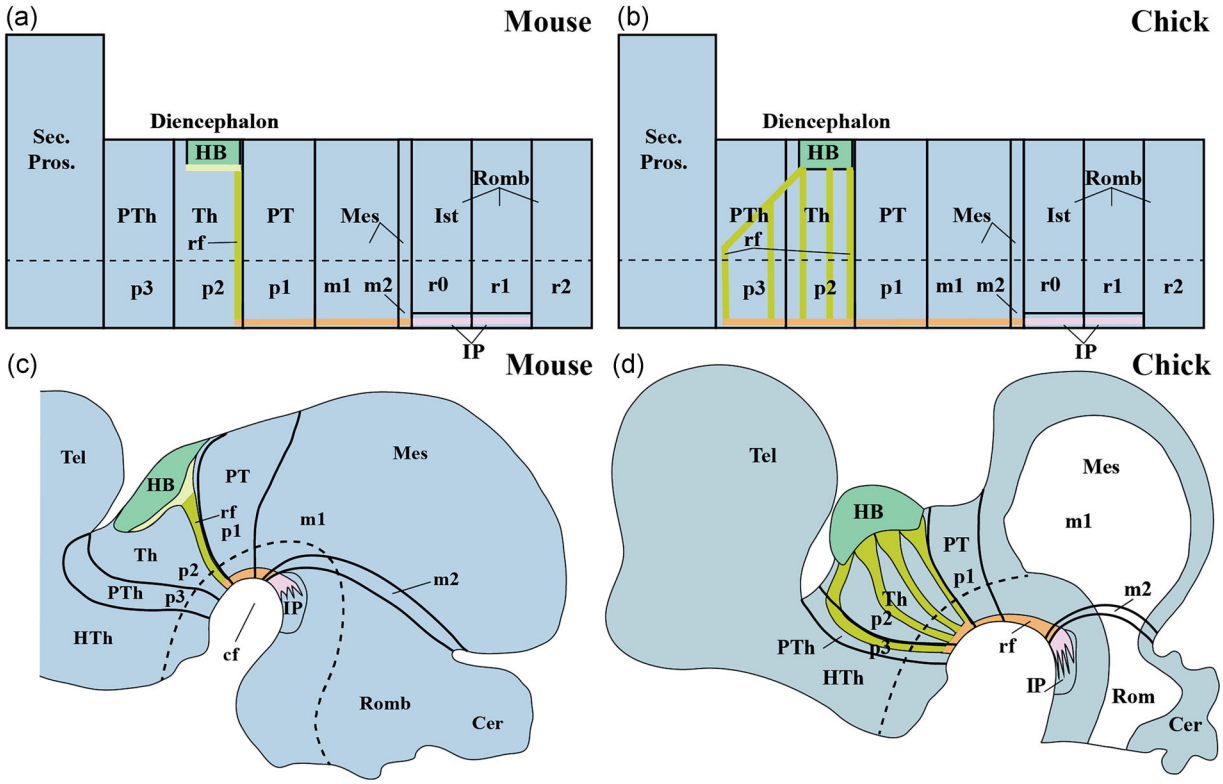

FIGURE 7 | Schema summarizing present results on the prosomere-related course of the retroflex tract in the mouse and chick in relatively abstract and realistic versions (a, c and /b, d, respectively). In contrast to the straightforward standard retroflex tract course seen in the mouse (a and b), the chick habenular efferent fibers (c and d) atypically penetrate an intermediate stratum of the thalamus territory, crossing it fan-shaped in a range of dorsoventral directions. The rostralmost fibers pass into the prethalamus, where they finish the dorsoventral course into the corresponding p3 tegmentum, in parallel to the less atypical transthalamic ones that only course through p2. The pretectum is not significantly invaded. The different retroflex fiber packets reach separately the paramedian basal area, perform independently analogous retroflexions at different rostrocaudal neuromeric locations, and collect in the pretectal and midbrain paramedian tegmentum before entering longitudinally the interpeduncular complex of the prepontine hindbrain. The peculiarity of this course would seem to be a consequence of the loss of the initial subhabenular trajectory that normally precludes entrance into the thalamic nuclear mass. It is unclear whether the presence of a nearly standard contingent of fibers jointly with the diverse atypical transthalamic contingents reveals a separation of core medial habenular fibers from the lateral habenular elements thought to form a shell around the core component. Habenulo-interpeduncular course into 4 parts named subhabenular (yellow), retrothalamic (green), tegmental (orange), and interpeduncular (pink).

the transverse thalamo-pretectal boundary (caudally to the ovoid mass of the thalamic primordium, barely contacting its intermediate and ventral tiers); this trajectory continues straight across the caudal p2 tegmentum until the fibers reach the paramedian part of the basal plate, next to the floorplate, where they sharply flex caudalwards.

3. *Tegmental course*: This part occurs after the tract's retroflexion and represents a paramedian longitudinal course backwards across the pretectal (p1) and midbrain (m1 and m2) tegmentum, until the fibers enter ipsilaterally the median interpeduncular nuclear complex of the prepontine hindbrain.

4. *Interpeduncular course*: This is the zigzagging rostrocaudal final course, repeatedly crisscrossing the whole midline of the interpeduncular complex along the isthmic and r1 regions and producing terminal synaptic connections within and outside the IP complex.

4.2 | Possible Causal Conditions of the Atypical Course of Chick Habenular Efferents

The causal determinants of these four different behaviors manifested in series by supposedly similar though essentially somewhat heterogeneous fibers (due to separate origins in distinct and by no means homogeneous medial and lateral habenular nuclei) remain largely unknown, though some recent progress has accrued (e.g., Company, Moreno-Cerdá et al. 2021; Company, Andreu-Cervera, et al. 2021; Company et al. 2022). It seems possible to ascribe tentatively some causal roles to different navigational conditions the fibers appear to find at each locus.

The subhabenular trajectory suggests that the habenular efferents preferentially sort individually out of the habenular complex itself before fasciculating together and elongating significantly caudalwards under the HB (they essentially exit individually out of the habenular complex following the shortest route from

their respective cell bodies). However, they apparently normally find that the subjacent thalamic medium is nonpermissive for their growth, which forces them to eschew entering the underlying thalamic mass and remain restricted to the longitudinal thalamo-subhabenular interstice. Their clear-cut preference for a *caudalwards course* at this subhabenular locus remains unexplained and unexamined (note the stria medullaris tract enters longitudinally the habenular area at its rostral end *but does not enter the subhabenular interstice*).

Once the subhabenular retroflex tract collects caudally under the differentially *Pax6*-positive retrohabenular area, its fibers largely are not able to continue their previous longitudinal course, which would bring them into the dorsal part of the pretectum. We saw a few *vertical* fibers that may be interpreted as having passed directly from the caudalmost HB into the adjoining rostral precommissural pretectum, where they course ventralwards separated from the standard retroflex tract (Figures 3a,b,d). However, the majority of longitudinal fibers possibly meet at this locus a different sort of nonpermissive signal (e.g., Funato, Saito-Nakazato, and Takahashi 2000), which prohibits entrance into the pretectum (the latter corresponds to a different neuromere, where a variant molecular profile rules local neurohistogenesis, as predicted by the prosomeric model (Ferran et al. 2007, 2008, 2009); no such explanation can be offered by the columnar model because it includes the rostral pretectum in the habenular/thalamic region; Figure 1a). Expelled both from the thalamus and the pretectum, the choice apparently gets reduced to coursing dorsoventrally along the back of the thalamus and in front of the pretectum, thus following the interprosomeric boundary ventralwards at least while crossing the alar plate. It is also an interesting aspect in mammals that this dorsoventral trajectory lies close to the periventricular stratum, indicating a possibly temporally coded molecular adhesive restriction versus more superficial radial strata. Nothing seems to impede subsequently the continuation of the same dorsoventral course across the underlying prerubral thalamic (p2) tegmentum at its interprosomeric boundary with the p1 tegmentum (in mammals, the retroflex fibers notoriously eschew penetrating here into the subpretectal tegmental area occupied by the parvocellular red nucleus, the nucleus of Darkschewitsch, and the interstitial nucleus of Cajal). However, further advance of the retroflex fibers along this dorsoventral tegmental trajectory meets another obstacle when they approach the local floorplate, which they normally do not seem able to approach and cross. Mice studies determined that Sema3F and Sema5A are involved in the establishment of a permissive corridor in front of the pretecto-thalamic boundary (Funato, Saito-Nakazato, and Takahashi 2000; Kantoretal et al. 2004). Diffusing NTN1 protein apparently attracts habenular efferent fibers to the basal plate (Funato, Saito-Nakazato, and Takahashi 2000), and SLIT2 protein works as a floorplate-originated repellent that impedes the crossing of the p2/p1 midline by retroflex tract fibers (Moreno-Bravo et al. 2016).

At this point, next to the FP, the fibers retroflect into their descending paramedian tegmental course (as noticed by Meynert 1872). Why they retroflect caudalwards and essentially do not turn rostralwards remains an obscure point (though mice devoid of some gene functions do produce rostrally coursing retroflex tract fibers at this locus, Moreno-Bravo et al. 2016). There is perhaps a gradient of attracting signals increasing across the midbrain tegmentum into the hindbrain that orients the fibers caudalwards, or the retroflexion decision is helped by some repellent signal placed rostrally in the diencephalic tegmentum, or both (see recent experimental data on retroflex tract guidance by Moreno-Bravo et al. 2016 and Company, Moreno-Cerdá et al. 2021; Company, Andreu-Cervera, et al. 2021; Company et al. 2022). The constant paramedian position of the ulterior tegmental course of the retroflex tract across pretectum and midbrain possibly bespeaks of a subtle attraction by the local floorplate neighborhood or local radial glia (which we have seen also express BEN; Figure 6c–f), or alternatively, an adhesive fasciculation with some other contingent of descending longitudinal basal fibers (though nothing specific about this possibility is known so far).

The final zigzagging course of the retroflex fibers through the interpeduncular complex as soon as the tract enters the hindbrain paramedian tegmentum is a pattern of terminal arborization that is unique in the brain (Bianco et al. 2008; Iwahori et al. 1993; Ramón y Cajal 1911). A complex signal/reaction mechanism would seem to be involved, probably caused essentially by local signals created inside the interpeduncular complex, including floorplate-derived ones (e.g., a long-range attractor plus a short-range repellent, and possible interactions with the contralateral fibers doing the opposite course). Some local midline signal possibly attracts both right and left fibers to approach orthogonally the midline, perhaps modulating by short-range floor repellence a growth impulse that lasts until the contralateral border of the nuclear complex is reached (in spite of contralaterally decreasing levels of the attracting signal as distance from the midline increases). Once at the lateral border of the complex, no more growth would be possible in that direction, and each fiber might be able to react again to a new cycle of approaching and bypassing the midline. Some additional causal element would be perhaps needed for achieving the steplike caudalwards advance obtained after each iterated midline crossing.

A different problem is posed by the potential selective synaptic targeting of particular interpeduncular subnuclei in order to establish specific connections. There are possibly up to a dozen IP subdivisions, considering differential isthmic and rostral/caudal r1 parts of the IP complex, each having several medio-lateral and dorsoventral subnuclei and a multiplicity of cell types migrated from different origins—alar and basal in different rhombomeres—with differential molecular profiles (Lorente-Cánovas et al. 2012). This synaptogenetic process is quite specific (e.g., SP-positive retroflex component fibers target specifically lateral, rostral, and rhabdoid subnuclei; Artymyshyn and Murray 1985; Contestabile et al. 1987). This would need a complex set of causal factors, unless a common origin for these particular IP subpopulations is disclosed. Moreover, some of the habenular axons synapse selectively on serotonergic, dopaminergic, and gabaergic neuronal populations outside the interpeduncular complex proper (e.g., Bueno et al. 2019; Metzger et al. 2021; Nishikawa et al. 1986). Given such final targeting diversity of its components, it is remarkable that the whole packet of habenular efferents remains tightly fasciculated in its approximation to the general target in the hindbrain. Indeed, only the hindbrain medium seems to favor their terminal de-fasciculation. Interestingly, it has been reported that efferents from the medial habenular nucleus form a central compact core within the tract, whereas the lateral habenular

efferents form a surrounding peripheral shell (Company, Moreno-Cerdá et al. 2021; Herkenham and Nauta 1979; LP, corroborating unpublished observations in reptiles).

Such tight fasciculation is clearly absent in the case of chick (avian) embryos, and the question arises whether the diverse observed atypical courses involve differentially the lateral habenular versus medial habenular efferent components (e.g., does one of these two fiber groups produce the "standard" retrothalamic component and the other the atypical transthalamic component?) This would perhaps suggest potential loss of their mutual core/shell fasciculating relationship as the root of the navigational difference (this point clearly requires additional study). In any case, the avian atypical fibers seem to lack (or are not able to obey) the standard nonpermissive signals we postulated may exist within the main thalamic cell mass. Instead of eschewing this cell mass and aggregating in the subhabenular and retrohabenular/retrothalamic interstices, in birds, most of the habenular efferents directly penetrate the thalamic mass and course through it in various directions. Only the caudalmost habenular fibers enter the standard retrothalamic course in front of the nonpermissive pretectum. It may be noticed in our Figure 1b that the habenulo-thalamic boundary or subhabenular interstice is not topologically transversal (i.e., interprosomeric), representing instead an *intraprosomeric longitudinal dorsoventral limit within* p2. The fact that in the chick many habenular fibers do penetrate the thalamus but not so the pretectum (p1) indicates that the respective thalamic and pretectal nonpermissive signals must act differently, and only the thalamic ones have been lost or are ineffective. In any case, the atypical habenular fibers s clearly prefer to grow into the thalamus, violating the intraprosomeric longitudinal habenulo-thalamic border, rather than proceeding into the standard subhabenular and retrothalamic course.

As regards the atypical transthalamic courses observed, a good number of them variously approach (first obliquely and then dorsoventrally) the thalamic tegmentum (i.e., the basal domain of the thalamic prosomere 2), but do so in a nonfasciculated dispersed pattern, at diverse angles, mainly passing through an intermediate radial stratum; this may be the only growth pattern available to these fibers within the thalamic mass. It may be recalled that dispersed transthalamic growth of habenulo-interpeduncular fiber packets also was observed in frogs (cited above). As regards these diverse dorsoventral courses, a strong ventral attraction originating either in the tegmentum or the FP would seem to be equally distributed, at least in p2 and p3, considering the atypical habenular fibers that grow first rostralward into the prethalamus. Indeed, a number of transthalamic fibers show longer rostroventral oblique courses, bringing them or not into the prethalamus before turning strictly ventralwards (are they also attracted by alar p3?). A number of them proceed strictly rostralwards and cross at various radial levels the interthalamic boundary, the ZLI intrathalamica of Rendahl, into prethalamus (Rendahl 1924; ZLI). This course brings them into the caudalmost part of the alar prethalamus (p3), whose domain is known to develop several anteroposterior progenitor subdomains, one of which might release an attractor (Puelles et al. 2020). However, these fibers hardly course in rostral direction within the prethalamus and immediately bend instead ventralwards parallel to the ZLI, shortly after having crossed this landmark. This dorsoventral course (captured in Figure 5f,g) resembles the standard retrothalamic one in occurring just in front of an interprosomeric boundary (here the ZLI; p3/p2) and behind the major alar nuclear derivatives of the local prosomere (prethalamic nuclei; see Figure 4d,e). The atypical habenular fibers that enter the prethalamus are thus immediately forced to grow ventralwards (in front of the ZLI and the thalamus). This transverse ventralwards course likewise invades without change in direction the underlying p3 tegmentum (as occurs in the standard course next to the p2/p1 boundary) and also includes a typical ipsilateral retroflexion of the course once the fibers reach a paramedian locus next to the floorplate. We did not observe any transprethalamic atypical fibers bending rostralwards into the neighboring peduncular HTh (Figure 1b). They uniformly course caudalwards (implying potentially similar molecularly coded decisions and local conditions as those that may contribute to the standard thalamic retroflexion decision farther caudal). These fibers soon meet the remaining counterparts in the p2 tegmentum. Here, they apparently gradually fasciculate together again (surprisingly indicating that they are still able to do so, after all, albeit outside an alar plate locus). Subsequently, they follow a standard joint course caudalwards through the pretectal and midbrain paramedian tegmentum, reaching finally the interpeduncular complex.

The atypical prethalamic route of some chick habenular efferents indicates, first, that the ZLI boundary permits an abnormal caudorostral crossing by the habenular fibers (either for the same reason that the transthalamic route is abnormally possible, or for other reasons). Second, the prethalamic mantle derivatives also seem to have in place nonpermissive signals impeding the free rostralward growth of these fibers once they enter the prethalamic mantle, irrespective that such preexistent signals would not have occasion to act in other vertebrates that lack these atypical habenular fibers. Third, these prethalamic signals obviously must be different from the thalamic ones (like the pretectal ones; this can also be tentatively explained by the differential molecular profile(s) of the p3 prosomere; Puelles et al. 2020).

These results on a manifestly possible analogous transprethalamic course of retroflex tract fibers in the chick go beyond what is known in frogs and suggest the possible existence of potential rules of axonal growth established as a consequence of neuromeric subdivisions (molecular boundaries and differential associated genoarchitectural properties) occurring within a specific proneuromere (note the early primordium of the Dien is held to be a forebrain proneuromere that subdivides secondarily into pretectal, thalamic, and prethalamic prosomeres [p1–p3]; Puelles 2018). The retroflex tract later simply progresses longitudinally across the mesencephalic forebrain proneuromere (m1 and m2) and ends in the rostralmost prepontine hindbrain proneuromere (encompassing r0, r1r, r1c subdivisions, which together form the IP complex; Lorente-Cánovas et al. 2012). It seems that the prosomeric model (Figure 1b) helps the causal understanding of both the standard retroflex course in its diverse sectors and its variants in the chick and frog. This contrasts with the apparent lack of whatsoever cogent explanations after an analysis of the same data under columnar model assumptions (Figure 1a).

The theoretical question may arise whether the variant avian retroflex tract is homologous to the retroflex tract in other vertebrates. The fact that both the origin and the targets of the tract remain essentially invariant in their topological location within the prosomeric Bauplan suggests that fundamental homology may be accepted. The partial variation in the course probably results functionally inconsequential in its main aspects, and its fitness value thus would not change significantly, thus becoming invisible to natural selection. However, it can be noted that the variant retroflex tract course observed in birds might introduce evolutionary novelty in the resulting circuitry if it happened that novel *en passant* connections emerge between the transthalamic fibers and the thalamic neurons or the trans-prethalamic fibers and prethalamic neurons (similar for the anomalous p3 tegmental neurons crossed by the atypical fibers). Such hypothetic potential novel contacts of the variant habenular efferents might turn out to be adaptive and have been selected as birds diverged evolutionarily from reptiles. This interesting possibility obviously needs further investigation, exploring any such atypical new synaptic contacts. We unfortunately ignore which ancestor of the chick first presented the variant course of this tract (a bird or a dinosaur?), but wide investigation in cladistic terms of hodologic or molecular habenulo-interpeduncular peculiarities among birds and relevant sister outgroups might illuminate this field of inquiry.

It is hoped that the present descriptive analysis establishes chick embryos as useful comparative material in the search of the molecular mechanisms guiding the variable course and potential functions of habenulo-interpeduncular fibers, preferably as examined here within the prosomeric model. The relevant standard retroflex course was systematized here into four distinct course components: subhabenular, retrothalamic, tegmental, and interpeduncular. Right angle bends (sharp navigational decisions) separate the first three trajectories, and the final interpeduncular zigzagging may be understood as a complex 180°-angle bend in series. In the chick case, the first course component seems specifically altered, causing variant invasive transthalamic dispersion of the tract fibers (and secondarily their diminished histological visibility), but the changed trajectories observed show some neuromere-related topological analogies, even in ways that involve invading an abnormal prosomere (a different diencephalic region), to finally, after several added course decision points, reach nevertheless the correct targets. This is accordingly also an interesting case of visible canalization or buffering of a developmental axonal navigational mechanism, revealing possible *preexisting* alternative signaling mechanisms that normally do not function (or have other functions) but can equally direct atypical axons into the *correct* target under some conditions.

Author Contributions

J.L.F. did the experiments. J.L.F. and L.P. analyzed the data, wrote, and revised the manuscript.

Acknowledgments

We are thankful to the Spanish Ministry of Science, Innovation and Universities (MCIU), State Research Agency (AEI) and European Regional Development Fund (FEDER) PGC2018-098229-B-100 to JLF) and by Séneca Foundation (19904/GERM/15 and 21903/PI/22) for the financial support.

Conflicts of Interest

The authors declare no conflicts of interest.

Data Availability Statement

All relevant data that support the findings are within the manuscript.

References

Alonso, A., P. Merchán, J. E. Sandoval, et al. 2012. "Development of the Serotonergic Cells in Murine Raphe Nuclei and Their Relations with Rhombomeric Domains." *Brain Structure and Function* 218: 1229–1277. https://doi.org/10.1007/s00429-019-02015-2013.

Artymyshyn, R., and M. Murray. 1985. "Substance P in the Interpeduncular Nucleus of the Rat: Normal Distribution and the Effects of Deafferentation." *Journal of Comparative Neurology* 231: 78–90. https://doi.org/10.1002/cne.902310107.

Bardet, S. M., I. Cobos, E. Puelles, M. Martínez-de-la-Torre, and L. Puelles. 2006. "The Chicken Lateral Septal Organ and Other Circumventricular Organs form in a Striatal Subdomain, Abutting the Molecular Striatopallidal Border." *Journal of Comparative Neurology* 499: 745–767.

Bayer, S. A., and J. Altman. 2004. "The Human Brain During the Third Trimester." In *Atlas of Human Central Nervous System Development*, Vol. 2, 1–392. Boca Raton, Florida: CRC Press.

Beccari, N. 1923. "Il Centro Tegmentale e Interstiziale ed Altre Formazioni Poco Note Nel Mesencéfalo en el Diencéfalo di un Rettile." *Italian Journal of Anatomy and Embryology* 20: 560–619.

Beccari, N. 1943. *Neurologia Comparata Anatomo-Funzionale Dei Vertebrati, Compreso l'Uomo*. Firenze: Sansoni.

Bianco, I. H., M. Carl, C. Russell, J. D. W. Clarke, S. W. Wilson. 2008. "Brain Asymmetry is Encoded at the Level of Axon Terminal Morphology." *Neural Development* 3: 9. https://doi.org/10.1186/1749-8104-3-9.

Bösel, R. 1974. "Das Erste Nervenfaserwachstum im Gehirn von Hühnerembryonen bis zum Stadium HH17." *Journal für Hirnforschung* 15: 23–48.

Bueno, D., L. B. Lima, R. Souza, et al. 2019. "Connections of the Laterodorsal Tegmental Nucleus with the Habenular-Interpeduncular-Raphe System." *Journal of Comparative Neurology* 527: 3046–3072. https://doi.org/10.1002/cne.24729.

Chédotal, A., O. Pourquié, and C. Sotelo. 1995. "Initial Tract Formation in the Brain of the Chick Embryo: Selective Expression of the BEN/SC1/DM-GRASP Cell Adhesion Molecule." *European Journal of Neuroscience* 7: 198–212. https://doi.org/10.1111/j.1460-9568.1995.tb01056.x.

Company, V., A. Moreno-Cerdá, A. Andreu-Cervera, et al. 2021. "Wnt1 Role in the Development of the Habenula and the Fasciculus Retroflexus." *Frontiers in Cell and Developmental Biology* 9: 755729. https://doi.org/10.3389/fcell.2021.755729.

Company, V., A. Andreu-Cervera, M. P. Madrigal, et al. 2021. "Netrin 1-Mediated Role of the Substantia Nigra Pars Compacta and Ventral Tegmental Area in the Guidance of the Medial Habenular Axons." *Frontiers in Cell and Developmental Biology* 9: 682067. https://doi.org/10.3389/fcell.2021.682067.

Company, V., R. Murcia-Ramón, A. Andreu-Cervera, et al. 2022. "Adhesion Molecule Amigo2 is Involved in the Fasciculation Process of the Fasciculus Retroflexus." *Developmental Dynamics* 251, no. 11: 1834–1847. https://doi.org/10.1002/dvdy.513.

Contestabile, A., L. Villani, A. Fasolo, et al. 1987. "Topography of Cholinergic and Substance P Pathways in the Habenulo-Interpeduncular System of the Rat. An Immunocytochemical and Microchemical approach." *Neuroscience* 21: 253–270. https://doi.org/10.1016/0306-4522(87)90337-X.

Dávila, J. C., S. Guirado, and L. Puelles. 2000. "Calcium-Binding Proteins in the Diencephalon of the Lizard *Psammodromus algirus*." *Journal of Comparative Neurology* 427: 67–92.

den Boer-Visser, A. M., M. L. Brittijn, and J. L Dubbeldam. 2004. *A Stereotaxic Atlas of the Brain of the Collared Dove, Streptopelia decaocto*. Shaker: Maastricht.

Diaz, C., L. Perez-Santana, M. Martinez-de-la-Torre, and L. Puelles. 1999. "Diencephalic Neuronal Populations Projecting Axons into the Basal Plate in a Lizard." *European Journal of Morphology* 37: 130–133. https://doi.org/10.1076/ejom.37.2.130.4734.

Díaz, C., and L. Puelles. 1992. "In vitro HRP-Labeling Experiments on the Connections of the Fasciculus Retroflexus in the Lizard *Gallotia gallotia*." *Brain Behavior and Evolution* 39: 305–311. https://doi.org/10.1159/000114127.

Díaz, C., C. Yanes, C. M. Trujillo, and L. Puelles. 1994. "The Lacertidian Reticular Thalamic Nucleus Projects Topographically Upon the Dorsal Thalamus: Experimental Study in *Gallotia galloti*." *Journal of Comparative Neurology* 343: 193–208. https://doi.org/10.1002/cne.903430202.

Edinger, L. 1908. *Vorlesungen über den Bau der Nervösen Zentralorgane des Menschen und der Tiere für Ärzte und Studierende. 2ter Band. Vergleichende Anatomie des Gehirns*, 7te Auflage. Leipzig: Verlag von FCW Vogel.

Ferran, J. L., L. Sánchez-Arrones, J. E. Sandoval, and L. Puelles. 2007. "A Model of Early Molecular Regionalization in the Chicken Embryonic Pretectum." *Journal of Comparative Neurology* 505, no. 4: 379–403. https://doi.org/10.1002/cne.21493.

Ferran, J. L., L. Sánchez-Arrones, S. M. Bardet, J. E. Sandoval, M. Martínez-de-la-Torre, and L. Puelles. 2008. "Early Pretectal Gene Expression Pattern Shows a Conserved Anteroposterior Tripartition in Mouse and Chicken." *Brain Research Bulletin* 75: 295–298. https://doi.org/10.1016/j.brainresbull.2007.10.039.

Ferran J. L., E. Dutra de Oliveira, L. Sánchez-Arrones, J. E. Sandoval, M. Martínez-de-la-Torre, and L. Puelles. 2009. "Genoarchitectonic Profile of Developing Nuclear Groups in the Chicken Pretectum." *Journal of Comparative Neurology* 517: 405–451. https://doi.org/10.1002/cne.22115.

Ferran, J. L., A. Ayad, P. Merchán, et al. 2015a. "Exploring Brain Genoarchitecture by Single and Double Chromogenic in Situ Hybridization (ISH) and Immunohistochemistry (IHC) in Whole-Mount Embryos." In *In Situ Hybridization Methods*, edited by G. Hauptmann, 61–82. New York, NY: Springer. https://doi.org/10.1007/978-1-4939-2303-8_4.

Ferran, J. L., A. Ayad, P. Merchán, et al. 2015b. "Exploring Brain Genoarchitecture by Single and Double Chromogenic in Situ Hybridization (ISH) and Immunohistochemistry (IHC) on Cryostat, Paraffin, or Floating Sections." In *In Situ Hybridization Methods*, edited by G. Hauptmann, 83–107. Berlin: Springer. https://doi.org/10.1007/978-1-4939-2303-8_5.

Freudenmacher, L., A. von Twickel, and W. Walkowiak. 2020. "The Habenula as an Evolutionary Conserved Link between Basal Ganglia, Limbic, and Sensory Systems—A Phylogenetic Comparison Based on Anuran Amphibians." *Journal of Comparative Neurology* 528: 705–728. https://doi.org/10.1002/cne.24777.

Funato, H., Y. Saito-Nakazato, and H. Takahashi. 2000. "Axonal Growth from the Habenular Nucleus Along a Neuromere Boundary Region of the Diencephalon is Regulated by Semaphorin 3F Andnetrin-1." *Molecular and Cellular Neuroscience* 16: 206–220. https://doi.org/10.1006/mcne.2000.0870.

García-Guillén, I. M., A. Alonso-Fuentes, N. Morales-Delgado, et al. 2020. "Netrin-1/DCC Signaling Differentially Regulates the Migration of Pax7, Nkx6.1, Irx2, Otp and Otx2 Cell Populations of the Developing Interpeduncular Nucleus." *Frontiers in Cell and Developmental Biology* 8: 1–11. https://doi.org/10.3389/fcell.2020.588851.

García-Guillén, I. M., A. Alonso, L. Puelles, F. Marín, and P. Aroca. 2021. "Multiple Regionalized Genes and Their Putative Networks in the Interpeduncular Nucleus Expose Complex Mechanisms of Neuron Development and Axon Guidance." *Frontiers in Neuroanatomy*, 15: 643320. https://doi.org/10.3389/fnana.2021.643320.

González, G., L. Puelles, and L. Medina. 2002. "Organization of the Mouse Dorsal Thalamus Based on Topology, Calretinin Immunostaining and Gene Expressions." *Brain Research Bulletin* 57: 439–443. https://doi.org/10.1016/S0361-9230(01)00720-1.

Groenewegen, H. J., S. Ahlenius, S. N. Haber, N. W. Kowall, and W. J. H. Nauta. 1986. "Cytoarchitecture, Fiber Connections, and Some Histochemical Aspects of the Interpeduncular Nucleus in the Rat." *Journal of Comparative Neurology* 249: 65–102. https://doi.org/10.1002/cne.902490107.

Guillén-Pérez, M. 1991. "Estructura del epitálamo y complejo superior del tálamo dorsal en aves: estudio embriológico y posibles homologías con mamíferos." Doctoral thesis, University of Murcia.

Hamburger, V., and H. L. Hamilton. 1951. "A Series of Normal Stages in the Development of the Chick Embryo." *Journal of Morphology* 88, no. 1: 49–92. Portico. https://doi.org/10.1002/jmor.1050880104.

Herkenham, M., and W. J. Nauta. 1979. "Efferent Connections of the Habenular Nuclei in the Rat." *Journal of Comparative Neurology* 187: 19–47. https://doi.org/10.1002/cne.901870103.

Herrick, C. J. 1910. "The Morphology of the Forebrain in Amphibia and Reptilia." *Journal of Comparative Neurology* 20: 413–547. https://doi.org/10.1002/cne.920200502.

Herrick, C. J. 1948. *The Brain of the Tiger Salamander, Ambystoma tigrinum*. Chicago: Univ. Chicago Press. https://doi.org/10.5962/bhl.title.6375.

Hidalgo-Sánchez, M., M. Martínez-de-la-Torre, R. M. Alvarado-Mallart, and L. Puelles. 2005. "Distinct Pre-Isthmic Domain, Defined by Overlap of *Otx2* and *Pax2* Expression Domains in the Chicken Caudal Midbrain." *Journal of Comparative Neurology* 483: 17–29.

His, W. 1893. "Über das frontale Ende des Gehirnrohres." *Arch Anat EntwGesch* 1893: 157–171.

His, W. 1895. Die Anatomische Nomenclatur. Nomina Anatomica, Neurologie. Arch. Anat. Entwickelungsges (Suppl.), 155–177.

His, W. 1904. *Die Entwicklung des Menschlichen Gehirns Während der Ersten Monaten*. Leipzig: Hirzel.

Huber, G. C., and E. C. Crosby. 1929. "The Nuclei and Fiber Paths of the Avian Diencephalon, with Consideration of Telencephalic and Certain Mesencephalic Centers and Connections." *Journal of Comparative Neurology* 48: 1–225. https://doi.org/10.1002/cne.900480102.

Iwahori, N., K. Nakamura, S. Kameda. 1993. "Terminal Patterns of the Fasciculus Retroflexus in the Interpeduncular Nucleus of the Mouse: A Golgi study." *Anatomy and Embryology* 187: 523–528. https://doi.org/10.1007/BF00214430.

Jiao, Y., L. Medina, C. L. Veenman, C. Toledo, L. Puelles, and A. Reiner. 2000. "The Anterior Nucleus of the Ansa Lenticularis in Birds is the Homologue of the Mammalian Subthalamic Nucleus." *Journal of Neuroscience* 20: 6998–7010. https://doi.org/10.1523/JNEUROSCI.20-18-06998.2000.

Kantor, D. B., O. Chivatakarn, K. L. Peer, et al. 2004. "Semaphorin 5A Is a Bifunctional Axon Guidance Cue Regulated by Heparan and Chondroitin Sulfate Proteoglycans." *Neuron* 44: 961–975. https://doi.org/10.1016/j.neuron.2004.12.002.

Kappers, C. U. A., G. C. Huber, and E. C. Crosby. 1936. *The Comparative Anatomy of the Nervous System of Vertebrates, including Man*. New York: The MacMillan Co.

Karten, H. J., and W. Hodos. 1967. *A Stereotaxic Atlas of the Brain of the Pigeon (Columba livia)*. Baltimore: The Johns Hopkins Univ. Press.

Kemali, M., and V. Braitenberg. 1969. *Atlas of the Frog's Brain*. Berlin: Springer Verlag.

Kemali, M., V. Guglielmotti, and D. Gioffré. 1980. "Neuroanatomical Identification of the Frog Habenular Connections Using Peroxydase

(HRP)." *Experimental Brain Research* 38: 341–347. https://doi.org/10.1007/BF00236654.

Kemali, M., and V. Guglielmotti. 1982. "The Connections of the Frog Interpeduncular Nucleus (ITP) Demonstrated with Horseradish Peroxydase (HRP)." *Experimental Brain Research* 45: 349–356. https://doi.org/10.1007/BF01208594.

Kemali, M., and G. Lázár. 1985. "Cobalt Injected into the Right and Left Fasciculi Retroflexes Clarifies the Organization of this Pathway." *Journal of Comparative Neurology* 233: 1–11. https://doi.org/10.1002/cne.902330102.

Kuenzel, W. J., and M. Masson. 1988. *A Stereotaxic Atlas of the Brain of the Chick (Gallus domesticus)*. Baltimore: The Johns Hopkins Univ. Press.

Kuhlenbeck, H. 1973. *The Central Nervous System of Vertebrates*, Vol. 3, Part II. Berlin: S.Karger A.G. https://doi.org/10.1159/isbn.978-3-318-05155-1.

Kuhlenbeck, H. 1977. *The Central Nervous System of Vertebrates*, Vol. 5, Part I. Berlin: S.Karger A.G. https://doi.org/10.1159/isbn.978-3-318-05157-5.

Lee, M., J. Yoon, H. Song, et al. 2017. "*Tcf7l2* Plays Crucial Roles in Forebrain Development through Regulation of Thalamic and Habenular Neuron Identity and Connectivity." *Developmental Biology* 424: 62–76. https://doi.org/10.1016/j.ydbio.2017.02.010.

Loonen, A. J. M., and S. A. Ivanova. 2016. "Circuits Regulating Pleasure and Happiness: The Evolution of the Amygdalar-Hippocampal-Habenular Connectivity in Vertebrates." *Frontiers in Neuroscience* 10: 539. https://doi.org/10.3389/fnins.2016.00539.

Lorente-Cánovas, B., F. Marín, R. Corral-San-Miguel, et al. 2012. "Multiple Origins, Migratory Paths and Molecular Profiles of Cells Populating the Avian Interpeduncular Nucleus." *Developmental Biology* 361: 12–26. https://doi.org/10.1016/j.ydbio.2011.09.032.

Lyser, K. 1966. "The Development of the Chick Embryo Diencephalon and Mesencephalon During the Initial Phases of Neuroblast Differentiation." *Journal of Embryology and Experimental Morphology* 16: 497–517. https://doi.org/10.1242/dev.16.3.497.

Medina, L., and A. Reiner. 1994. "Distribution of Choline Acetyltransferase Immunoreactivity in the Pigeon Brain." *Journal of Comparative Neurology* 342, no. 4: 497–537. Portico. https://doi.org/10.1002/cne.903420403.

Martínez-de-la-Torre, M., A.-L. Garda, E. Puelles, and L. Puelles. 2002. "*Gbx2* Expression in the Late Embryonic Chick Dorsal Thalamus." *Brain Research Bulletin* 57: 435–438. https://doi.org/10.1016/S0361-9230(01)00721-3.

Merchán, P., S. M. Bardet, L. Puelles, and J. L. Ferran. 2011. "Comparison of Pretectal Genoarchitectonic Pattern between Quail and Chicken Embryos." *Frontiers in Neuroanatomy* 5: 23. https://doi.org/10.3389/fnana.2011.00023.

Metzger, M., R. Souza, L. B. Lima, et al. 2021. "Habenular Connections with the Dopaminergic and Serotonergic System and their Role in Stress-Related Psychiatric Disorders." *European Journal of Neuroscience* 53: 65–88. https://doi.org/10.1111/ejn.14647.

Meynert, T. H. 1872. *The Brain of Mammals (Transl. by J.J.Putnam), in Stricker S. "Manual of Histology"*, 650–766. New York: W.Wood Co.

Milán, J., and L. Puelles. 2000. "Patterns of Calretinin, Calbindin and Tyrosine-Hydroxylase Immunoreactivity Patterns are Consistent with the Prosomeric Map of the Frog Diencephalon." *Journal of Comparative Neurology* 419: 96–121. https://doi.org/10.1002/(SICI)1096-9861(20000327)419:1⟨96::AID-CNE6⟩3.0.CO;2-V.

Moreno-Bravo, J. A., A. Perez-Balaguer, J. E. Martinez-Lopez, et al. 2014. "Role of *Shh* in the Development of Molecularly Characterized Tegmental Nuclei in Mouse Rhombomere 1." *Brain Structure and Function* 219: 777–792. https://doi.org/10.1007/s00429-013-0534-6.

Moreno-Bravo, J. A., J. E. Martínez-López, P. Madrigal, et al. 2016. "Developmental Guidance of the Retroflex Tract at its Bending Point Involves Robo1-Slit2-Mediated Floor Plate Repulsion." *Brain Structure and Function* 221: 665–678. https://doi.org/10.1007/s00429-014-0932-4.

Nieuwenhuys, R., H. J. ten Donkelaar, and C. Nicholson. 1998. *The Central Nervous System of Vertebrates*, Vols. 1–3. Berlin: Springer.

Nieuwenhuys, R., and L. Puelles. 2016. *Towards a New Neuromorphology*. Berlin: Springer Verlag. https://doi.org/10.1007/978-3-319-25693-1.

Nishikawa, T., D. Fage, and B. Scatton. 1986. "Evidence for, and Nature of, the Tonic Inhibitory Influence of Habenulointerpeduncular Pathways Upon Cerebral Dopaminergic Transmission in the Rat." *Brain Research* 373: 324–336. https://doi.org/10.1016/0006-8993(86)90347-1.

Palmgren, A. 1921. "Embryological and Morphological Studies on the Midbrain and Cerebellum of Vertebrates." *Acta Zoologica (Stockh)* 2: 1–94. https://doi.org/10.1111/j.1463-6395.1921.tb00464.x.

Paxinos, G., T. M. Furlong, K. Ashwell, K. Smith, E. Calabrese, and G. A. Johnson. 2023. *MRI/DTI Atlas of the Human Brainstem in Transverse and Sagittal Planes*. London: Academic Press.

Pombal, M. A., and L. Puelles. 1999. "A Prosomeric Map of the Lamprey Forebrain Based on Calretinin Immunocytochemistry, Nissl Stain and Ancillary Markers." *Journal of Comparative Neurology* 414: 391–422. https://doi.org/10.1002/(SICI)1096-9861(19991122)414:3⟨391::AID-CNE8⟩3.0.CO;2-O.

Pourquié, O., M. Coltey, J. L. Thomas, N. M. Le Douarin. 1990. "A Widely Distributed Antigen Developmentally Regulated in the Nervous System." *Development* 109: 743–752. https://doi.org/10.1242/dev.109.4.743.

Puelles, L. 2001. "Thoughts on the Development, Structure, and Evolution of the Mammalian and Avian Telencephalic Pallium." *Philosophical Transactions of the Royal Society B: Biological Sciences (London)* 356: 1583–1598. https://doi.org/10.1098/rstb.2001.0973.

Puelles, L. 2013. "Plan of the Developing Vertebrate Nervous System Relating Embryology to the Adult Nervous System (Prosomere Model, Overview of Brain Organization)." In *Comprehensive Developmental Neuroscience: Patterning and Cell Type Specification in the Developing CNS and PNS*, edited by J. L. R. Rubenstein and P. Rakic, 187–209. Amsterdam: Academic Press.

Puelles, L. 2016. "Comments on the Limits and Internal Structure of the Mammalian Midbrain." *Anatomy [International Journal of Experimental and Clinical Anatomy]* 10: 60–70. https://doi.org/10.2399/ana.15.045.

Puelles, L. 2018. "Developmental Studies of Avian Brain Organization." *International Journal of Developmental Biology* 62: 207–224. https://doi.org/10.1387/ijdb.170279lp.

Puelles, L. 2019. "Survey of Midbrain, Diencephalon, and Hypothalamus Neuroanatomic Terms Whose Prosomeric Definition Conflicts with Columnar Tradition." *Frontiers in Neuroanatomy* 13: 20. https://doi.org/10.3389/fnana.2019.00020.

Puelles, L., and M. Martínez de la Torre. 1987. "Autoradiographic and Golgi Study on the Early Development of N. Isthmi Principalis and Adjacent Grisea in the Chick Embryo: A Tridimensional Viewpoint." *Anatomy and Embryology* 176: 19–34.

Puelles, L., and J. L. R. Rubenstein. 1993. "Expression Patterns of Homeobox and Other Putative Regulatory Genes in the Embryonic Mouse Forebrain Suggest a Neuromeric Organization." *Trends in Neurosciences* 16: 472–479. https://doi.org/10.1016/0166-2236(93)90080-6.

Puelles, L., and L. Medina. 1994. "Development of Neurons Expressing Tyrosine Hydroxylase and Dopamine in the Chicken Brain: A Comparative Segmental Analysis." In *Phylogeny and Development of Catecholamine Systems in the CNS of Vertebrates*, edited by A. Reiner and W. J. A. J. Smeets, 381–406. Cambridge: Cambridge University Press.

Puelles, L., and J. L. R. Rubenstein. 2003. "Forebrain Gene Expression Domains and the Evolving Prosomeric Model." *Trends in Neurosciences* 26: 469–476. https://doi.org/10.1016/S0166-2236(03)00234-0.

Puelles, L., and J. L. R. Rubenstein. 2015. "A New Scenario of Hypothalamic Organization: Rationale of New Hypotheses Introduced in the

Updated Prosomeric Model." *Frontiers in Neuroanatomy* 9: 27. https://doi.org/10.3389/fnana.2015.00027.

Puelles, L., F. J. Milán, and M. Martínez-de-la-Torre. 1996. "A Segmental Map of Subdivisions in the Diencephalon of the Frog *Rana Perezi*: Acetylcholinesterase-Histochemical Observations." *Brain Behavior and Evolution* 47: 279–310. https://doi.org/10.1159/000113248.

Puelles, L., M. Martínez-de-la-Torre, G. Paxinos, C. Watson, and S. Martínez. 2007. *The Chick Brain in Stereotaxic Coordinates: An Atlas Featuring Neuromeric Subdivisions and Mammalian Homologies*. San Diego: Elsevier/Academic Press.

Puelles, L., C. Watson, M. Martinez-de-la-Torre, and J. L. Ferran. 2012. "Diencephalon." In *The Mouse Nervous System*, edited by C. Watson, G. Paxinos, and L. Puelles, 313–336. Cambridge: Academic Press/Elsevier.

Puelles E., M. Martinez-de-la-Torre, C. Watson, L. Puelles. 2012. "Midbrain." In *The Mouse Nervous System*, edited by C. Watson, G. Paxinos, and L. Puelles, 337–359. Cambridge: Academic Press/Elsevier.

Puelles, L. 2021. "Recollections on the Origins and Development of the Prosomeric Model." *Frontiers in Neuroanatomy* 15. https://doi.org/10.3389/fnana.2021.787913.

Puelles, L., M. Martinez-de-la-Torre, S. Bardet, and J. L. R. Rubenstein. 2012 "Hypothalamus." In *The Mouse Nervous System*, edited by C. Watson, G. Paxinos, and L. Puelles, 221–312. Cambridge: Academic Press/Elsevier.

Puelles, L., M. Harrison, G. Paxinos, and C. Watson. 2013. "A Developmental Ontology for the Mammalian Brain Based on the Prosomeric Model." *Trends in Neurosciences* 36: 570–578. https://doi.org/10.1016/j.tins.2013.06.004.

Puelles, L., B. Fernández, and M. Martinez-de-la-Torre. 2015. "Neuromeric Landmarks in the Rat Midbrain, Diencephalon, and Hypothalamus, Compared with Acetylcholinesterase Histochemistry." In *The Rat Nervous System*, edited by G. Paxinos, 4th Edition, 25–43. New York: Academic Press/Elsevier.

Puelles, L., M. Martinez-de-la-Torre, S. Martinez, C. Watson, and G. Paxinos. 2019. *The Chick Brain in Stereotaxic Coordinates and Alternate Stains*, 2nd Edition. New York: Academic Press.

Puelles, L., C. Diaz, T. Stühmer, J. L. Ferran, M. Martínez-de la Torre, and J. L. R. Rubenstein. 2020. "LacZ-reporter Mapping of Dlx5/6 Expression and Genoarchitectural Analysis of the Postnatal Mouse Prethalamus." *Journal of Comparative Neurology* 529: 367–420. https://doi.org/10.1002/cne.24952.

Puelles, L., and M. Hidalgo-Sánchez. 2023. "The Midbrain Preisthmus: A Poorly Known Effect of the Isthmic Organizer." *International Journal of Molecular Sciences* 24, no. 11: 9769. https://doi.org/10.3390/ijms24119769.

Ramón y Cajal, S. 1911. *Histologie du Systeme Nerveux de l'Homme et des Vertebrés*, Vol. II. Madrid: CSIC. (1952 reprint of the revised French Edition, translated by L Azoulay).

Redies, C., K. Arndt, and M. Ast. 1997. "Expression of the Cell Adhesion Molecule Axonin-1 in Neuromeres of the Chicken Diencephalon." *Journal of Comparative Neurology* 381: 230–252. https://doi.org/10.1002/(SICI)1096-9861(19970505)381:2⟨230::AID-CNE9⟩3.0.CO;2-4.

Redies, C., M. Ast, S. Nakagawa, M. Takeichi, M. Martínez-de-la-Torre, and L. Puelles. 2000. "Morphologic Fate of Diencephalic Prosomeres and Their Subdivisions Revealed by Mapping Cadherin Expression." *Journal of Comparative Neurology* 421: 481–514. https://doi.org/10.1002/(SICI)1096-9861(20000612)421:4⟨481::AID-CNE3⟩3.0.CO;2-H.

Rendahl, H. 1924. "Embryologische Und Morphologische Studien über das Zwischenhirn beim Huhn." *Acta Zoologica (Stockh)* 5: 241–344. https://doi.org/10.1111/j.1463-6395.1924.tb00169.x.

Sánchez-Guardado, L. Ó., M. Irimia, L. Sánchez-Arrones, et al. 2011. "Distinct and Redundant Expression and Transcriptional Diversity of Meis Gene Paralogs During Chicken Development." *Developmental Dynamics* 240: 1475–1492. https://doi.org/10.1002/dvdy.22621.

Schmidt, E. R. E., S. Brignani, Y. Adolfs, et al. 2014. "Subdomain-Mediated Axon-Axon Signaling and Chemoattraction Cooperate to Regulate Afferent Innervation of the Lateral Habenula." *Neuron* 83: 372–387. https://doi.org/10.1016/j.neuron.2014.05.036.

Swanson, L. W. 1998. *Brain Maps: Structure of the Rat Brain*, 2nd Edition. Ámsterdam/Oxford: Elsevier.

Swanson, L. W. 2012. *Brain Architecture. Understanding the Basic Plan*, 2nd Edition. Oxford: Oxford Univ. Press.

Tello, J. F. 1924. "Les différenciations neuronales dans l'embryon de poulet pendant les premiéres jours de l'incubation." *Trav Lab Rech Biol (Madrid)* 21: 1–93.

Vaage, S. 1969. "The Segmentation of the Primitive Neural Tube in Chick Embryos (*Gallus domesticus*)." *Ergeb Anat Entwicklungsgesch* 41: 1–88.

Vaage, S. 1973. "The Histogenesis of the Isthmic Nuclei in Chick Embryos (*Gallus domesticus*). I. A Morphological Study." *Z Anat Entwickl Gesch* 142: 283–314. https://doi.org/10.1007/BF00519134.

Watson, C., T. Shimogori, and L. Puelles. 2017a. "Mouse FGF8-Cre Lineage Analysis Defines the Territory of the Postnatal Mammalian Isthmus." *Journal of Comparative Neurology* 525: 2782–2799. https://doi.org/10.1002/cne.24242.

Watson, C., A. Mitchelle, and L. Puelles. 2017b. "A new Mammalian Brain Ontology Based on Developmental Gene Expression." In *Evolution of Nervous Systems 2e*, edited by J. Kaas, Vol. 2, 53–75. Oxford: Elsevier.

Watson, C., M. Kirkcaldie, and L. Puelles. 2017. "Developmental Gene Expression Redefines the Mammalian Brain Stem." In *Evolution of Nervous Systems 2e*, edited by J. Kaas, Vol. 2, 467–475. Oxford: Elsevier.

Watson, C., C. Bartholomaeus, and L. Puelles. 2019. "Time for Radical Changes in Brain Stem Nomenclature—Applying the Lessons from Developmental Gene Patterns." *Frontiers in Neuroanatomy* 13: 10. https://doi.org/10.3389/fnana.2019.00010.

Windle, W. F., and M. F. Austin. 1936. "Neurofibrillar Development in the Central Nervous System of Chick Embryos Up to 5 Days' Incubation." *The Journal of Comparative Neurology* 63, 431–463. https://doi.org/10.1002/cne.900630304.

Yoon, M.-Y., L. Puelles, and C. Redies. 2000. "Formation of Cadherin-Expressing Brain Nuclei in Diencephalic Alar Plate Divisions." *Journal of Comparative Neurology* 421: 461–480. https://doi.org/10.1002/(SICI)1096-9861(20000612)421:4⟨461::AID-CNE2⟩3.0.CO;2-M.

Zweers, G. A. 1971. *A Stereotaxic Atlas of the Brainstem of the Mallard (Anas platyrhynchos)*. Assen: Koninklijke Van Gorcum & Comp.